Science of the Total Environment 657 (2019) 746–763

Contents lists available at ScienceDirect

Science of the Total Environment

journal homepage: www.elsevier.com/locate/scitotenv

Storylines of combined future land use and climate scenarios and their hydrological impacts in an Alpine catchment (Brixental/Austria)

Ulrich Strasser [a,*], Kristian Förster [b], Herbert Formayer [c], Florentin Hofmeister [a], Thomas Marke [a], Gertraud Meißl [a], Imran Nadeem [c], Rike Stotten [d], Markus Schermer [d]

[a] University of Innsbruck, Department of Geography, Innsbruck, Austria
[b] Leibniz Universität Hannover, Institute of Hydrology and Water Resources Management, Hannover, Germany
[c] BOKU University of Natural Resources and Life Sciences, Institute of Meteorology, Vienna, Austria
[d] University of Innsbruck, Department of Sociology, Innsbruck, Austria

HIGHLIGHTS

- We have combined scenarios of climate and land use change to so-called "storylines" of future local development
- Local experts from various societal sectors and scientists organized themselves in a mutual learning alliance
- A numerical hydrological model was used to quantify the effects of the storylines on the local water cycle
- A new version of the open-source hydrological model WaSiM is developed, including snow-canopy interaction processes

GRAPHICAL ABSTRACT

Inter- and transdisciplinary development of storylines of combined future land use and climate scenarios and their hydrological impacts in an Alpine catchment.

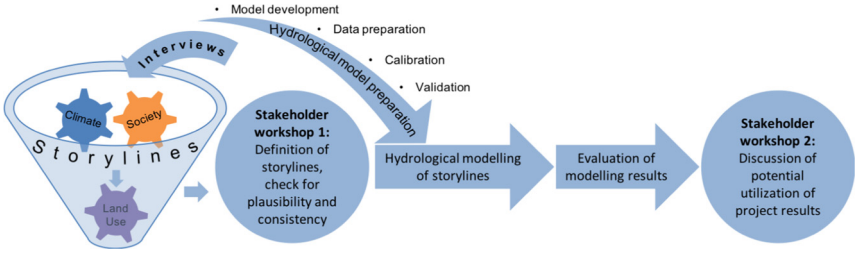

ARTICLE INFO

Article history:
Received 13 July 2018
Received in revised form 3 December 2018
Accepted 5 December 2018
Available online 8 December 2018

Editor: Ralf Ludwig

Keywords:
Mountain hydrology
Regional catchment
Land use
Climate change
Numerical modelling
Storyline development

ABSTRACT

In this paper, the hydrological impacts of future socio-economic and climatic development are assessed for a regional-scale Alpine catchment (Brixental, Tyrol, Austria). Therefore, coupled storylines of future land use and climate scenarios were developed in a transdisciplinary stakeholder process by means of questionnaire analyses and interviews with local experts from various relevant societal sectors. Resulting future land use maps for each decade were used as spatial input in the hydrological model WaSiM, to which a new module for the consideration of snow-canopy interaction processes has been added. Simulation results for three developed storylines, each combined with a moderate (A1B) and an extreme (RCP8.5) climate future, show that in a warmer and dryer climate the amount of annual simulated streamflow at the gauge of the catchment undergoes a significant reduction. The (mainly natural) reforestation of the catchment – caused by abandonment of previously cultivated areas – leads to additional losses of water by enhanced interception and evapotranspiration processes. Further cultivation of the current mountain pasture areas has a certain potential to attenuate undesirable long-term impacts of climate change on the catchment water balance.

© 2018 Elsevier B.V. All rights reserved.

1. Introduction

The Intergovernmental Panel on Climate Change IPCC has provided the SRES (Special Report on Emission Scenarios) climate scenarios (Nakicenovic and Swart, 2000) in 2000, which were superseded by

* Corresponding author.
E-mail address: ulrich.strasser@uibk.ac.at (U. Strasser).

https://doi.org/10.1016/j.scitotenv.2018.12.077
0048-9697/© 2018 Elsevier B.V. All rights reserved.

four greenhouse gas concentration trajectories in 2011 (the Representative Concentration Pathways, "RCPs") (Van Vuuren et al., 2011), adopted for the 5th assessment report. All these simulations of the global climate future are based on assumed developments of socio-economic conditions, land use and resulting greenhouse gas emissions. However, at the local scale the development of socio-economic patterns and land use may deviate from the global scenarios depending on a variety of natural (e.g. climatic conditions, topography) and societal (e.g. cultural and political framework) factors. As land use and its development over time strongly control the water cycle and runoff response of catchments to precipitation events, an estimate of potential future land use and its resulting hydrological impacts is valuable for responsible (i) planning of water demand and supply, (ii) operation of hydroelectric power stations and (iii) assessment of flood risk.

Changes in land cover are in general determined by the natural conditions such as climatic, topographic, geological and soil characteristics. A shift of the tree line induced by a changing climate is a prominent example for a land cover change enabled by new environmental conditions (Köplin et al., 2013). Locally, the land cover type is controlled by socio-economic factors and the development of new technological solutions (and called "land use" then). The socio-economic framework and new technological possibilities may have effects on shorter time scales than changes of the natural conditions. Major influencing factors for man-controlled agricultural and forest land use are the labor availability and its potential substitution by technical means. The mountainous Province of the Tyrol, where approximately only 11% of the land area can be used for permanent settlement, industry, traffic and infrastructure (Federal Province of Tyrol, 2017), is prone to overlapping uses and resulting conflicts. Developments in other sectors directly or indirectly affect agricultural land use and forest management by competition for labor or changing demand patterns for products like food, energy and timber (Tasser et al., 2012).

Land use change is well known to affect the hydrological response of a catchment, i.e. the flood mitigation effect of a forest (Wahren et al., 2012) or the effect of the vegetation type on evapotranspiration amount (Calder, 1993). Numerous modelling exercises exist to quantitatively assess the role of land use in the separation of the hydrological fluxes (e.g., Dunn and Mackay, 1995; Klöcking and Haberlandt, 2002; Cuo et al., 2009). However, only few studies attempt to combine both changing land use with changing climatic conditions for the future, and to quantify their relative effects on the hydrological system. The co-evolution of land use and climate is thereby mostly decoupled, and more or less simple assumptions are made for the local socio-economic and, depending on these, land use scenarios. E.g., Lahmer et al. (2001) investigated land use and climate change impacts for two mesoscale river catchments in Germany. Their results demonstrate that moderate land use changes result in only small changes of the water balance components, and larger effects could only be achieved by reforestation of larger agricultural areas. Zierl and Bugmann (2005) combined IPCC SRES scenarios of climate development with scenarios of socio-economic and land use change, based on the same IPCC SRES storylines as the climate scenarios (Ewert et al., 2005; Reginster and Rounsevell, 2003), to force a hydrological model. They found that „at the regional level afforestation is simulated to reduce annual runoff, while deforestation is simulated to increase annual runoff". The reasons were changes in transpiration, evaporation of intercepted water and sublimation of intercepted snow. The reduction of runoff was of subordinate importance compared to runoff changes introduced by climate change. Köplin et al. (2013) analyzed 15 mountainous catchments in Switzerland with different degrees of forest cover increase under scenarios of change. Confirming the results by Gasser et al. (2003) for the Thur catchment they found that runoff is reduced when forest area increases, but this reduction is not comparable in its magnitude to the change introduced by climate change. The effect of forestation only becomes crucial if extreme scenarios are assumed with forest increase of >35% of the catchment area, or if solely evapotranspiration is concerned (Köplin et al., 2013). Likewise, the sensitivity study of Tomer and Schilling (2009) shows the generally larger effect of the climate change signal on runoff compared to the land use change signal.

Apart from the assumptions for future land use development made in these studies, still little knowledge exists on a plausible and consistent co-evolution of local land use, according to the global socio-economic development, that goes along with the future climate scenarios. Therefore, in our study bottom-up generated socio-economic scenarios in combination with climate scenarios serve as a basis for hydrological modelling of streamflow in a defined catchment area. The storylines we define here represent different combinations of socio-economic trends and downscaled future climate scenarios for a specific hydrological catchment. The aims of our study hence are (i) to jointly generate storylines of socio-economic and climatic development at the local to regional scale that result in specific land use patterns, (ii) to model and evaluate their hydrological effects and (iii) to translate and communicate the simulated potential future socio-economic and hydrological effects to the community of the stakeholders.

In the section on the method of participatory local scenario development we show – building on the methodology of Kröger and Schäfer (2016) – that scenario development has the potential to serve as a tool for transdisciplinary integration. Shared knowledge production and mutual learning do not only occur among different disciplines, but also between scientists and non-scientists such as practitioners and decision makers. We further point out that the storylines are based on plausible and internally consistent assumptions about the evolution of key social and economic drivers. They can provide concrete illustrations or a possible future development and may result in tangible measures for adaptation to climate change, launched by the participating stakeholders themselves.

In the hydrological modelling section we present a new snow-canopy interaction module which we developed to enable a proper consideration of the combined effects of changing forested areas and precipitation regimes on the water fluxes (Förster et al., 2018). This new module has been integrated in the physically-based hydrological model WaSiM (Schulla, 1997, 2015) which we applied forced by three different storylines of potential land cover evolution, each for A1B and RCP8.5 future climate conditions. The model results show how the changing land use can attenuate or intensify the effects of a changing climate on the components of the water balance. As linear trends suggest linearity in change, we prefer to present and discuss changes in climatic and hydrological conditions with consideration of decadal variations in our analyses, in order to account for the distinct variability in the underlying data.

Our results can provide a basis for local decision makers for future land use planning and water management. Since WaSiM is an open source model, the new version of the code will be made available to the public (see www.wasim.ch/en/index.html).

2. Study site and data

The study site is the Brixental, the hydrological catchment of the Brixentaler Ache (322 km^2, discharge gauge at Bruckhäusl; Fig. 1). It is located in the East of the Federal province of the Tyrol (Austria) in the Kitzbüheler Alps north of the main ridge of the Eastern Alps in the Greywacke zone. The Brixental is a representative Alpine catchment, it is intensively used (forestry, pasturing, tourism, hydropower generation) and numerous stakeholders from various societal sectors are affected by changing land use, climate, and hydrology. Altitude ranges from 525 m a.s.l. at the gauge at Bruckhäusl to 2494 m a.s.l. at the highest point of the catchment, the summit of the Torhelm. Settlements are concentrated in the main valley, including the political municipalities of Brixen im Thale, Westendorf and Hopfgarten im Brixental as well as parts of Itter, Kirchbichl, and Wörgl. The land cover in the catchment is dominated by grassland and mainly coniferous forests, conifers with spruce being the prevalent tree species. Larch trees, firs, mountain pines, gray and green alders occur in smaller proportion. Forests would

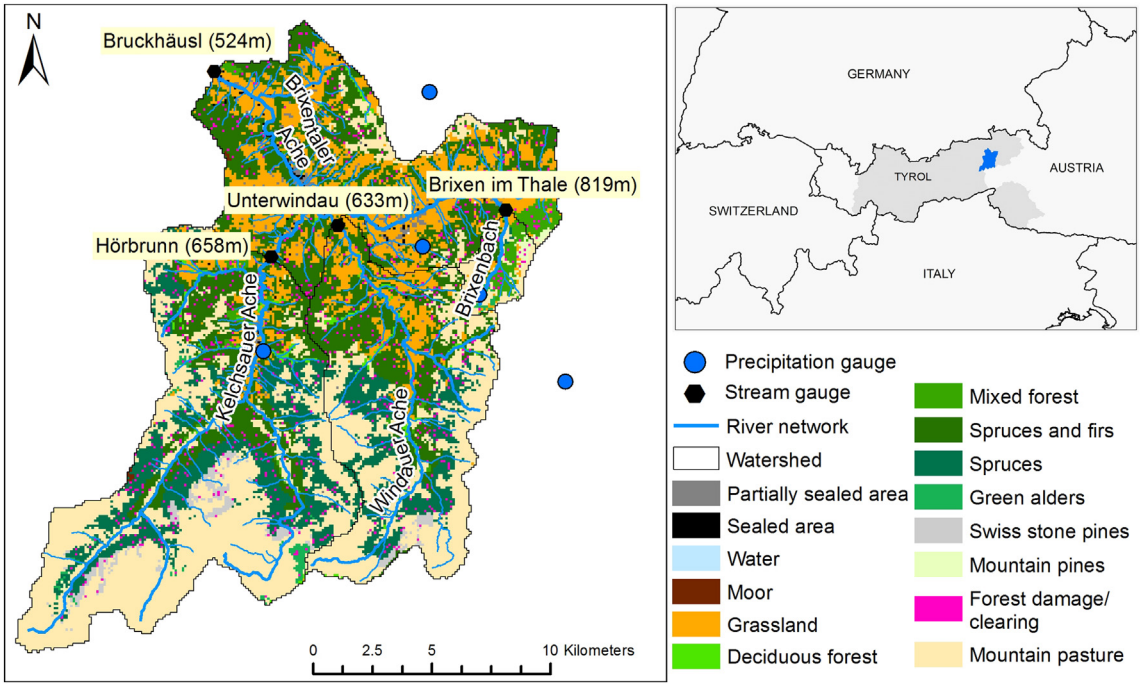

Fig. 1. The catchments Brixentaler Ache, Kelchsauer Ache, Windauer Ache and Brixenbach with precipitation and stream gauges, operated by the Hydrographic Service of Tyrol (2018). Land use based on the data set of the Federal Province of Tyrol (Federal Province of Tyrol, 2012) and the Schiechtl/Stern Forest map (Federal Province of Tyrol, 2009).

potentially cover the area up to the highest ridges, but the present tree line has been artificially lowered to give place for mountain pastures. Forest re-growth can be observed in many areas due to extensification of Alpine pastures (Tasser et al., 2007). The mean annual precipitation sum is about 1400 mm (measured at the precipitation gauge Am Nachtsöllberg, 990 m a.s.l.).

The hydrological catchment area covers the tributaries of the Kelchsauer Ache (134 km^2, discharge gauge at Hörbrunn), the Windauer Ache (82 km^2, discharge gauge at Unterwindau) and the Brixenbach (9 km^2, discharge gauge at Brixen im Thale). The streamflow gauges as well as several precipitation gauges are operated by the Hydrographic Service of Tyrol (2018). The discharge gauges Hörbrunn and Bruckhäusl are influenced by small river power plants, indicating the economic importance of water in the catchment.

The meteorological variables required by the hydrological model are precipitation, temperature, relative humidity, global radiation and wind speed. To provide these meteorological variables for validation and calibration we used the INCA data set of the ZAMG (Haiden et al., 2011). Temporal and spatial resolution of this data is 1 h and 1 km^2, respectively. It covers the period 2003–2016. Since INCA is an analysis product, its quality continuously improves in the course of this period.

A map of the grain size distribution of the soil as required as input to the hydrological model was derived from the substratum map of the Forestry Service of the Federal Province of Tyrol (Hotter et al., 2015). Land use information is based on the land use data set of the Federal Government of Tyrol (Federal Province of Tyrol, 2012) with slight modifications, e.g. forests were distinguished into broad-leaved, mixed and coniferous, based on the map of Schiechtl and Stern (Federal Province of Tyrol, 2009).

The digital terrain model ALS-DTM was produced with Airborne Laserscanning data from 2008 to 2009 by the Federal Province of the Tyrol (2018). All spatial data used for the WaSiM simulations were resampled to a resolution of 50 m.

3. Methods

The combined evolution of socio-economic and climatic conditions is crucial to project local developments of future land use. For this study, local storylines for possible future developments of land use and climate were constructed in a participatory, inter- and transdisciplinary process with stakeholders from the region investigated. The resulting six storylines prepared for the hydrological modelling were selected out of the entire set of combinations of six socio-economic scenarios and two climatic scenarios.

3.1. Climate scenarios

Two different local climate change scenarios have been bias-corrected and localized for the study region. One, the CNRM_ARPEGE-RM5.1_ALADIN_25km_A1B scenario (further on “A1B”), is based on the SRES A1B emission scenario (Nakicenovic and Swart, 2000) which corresponds to an intermediate increase of greenhouse gases in the 21st century. With respect to CO_2 concentration, radiative forcing and temperature response in the newer IPCC RCPs, the A1B emission scenario corresponds to RCP6.0, approximately (Van Vuuren and Carter, 2014). The other, the BOKU_GFDL-CM3_WRF_10km_RCP8.5 scenario (further on “RCP8.5”), is based on the RCP8.5 scenario (Van Vuuren et al., 2011) which corresponds to a strong increase of greenhouse gases in the 21st century. These two datasets have a different origin, but provide a suitable basis to be appropriately communicated to the stakeholders as “moderate” and “extreme” climate futures in the investigated region. Of course, the two communicated climate futures are only a selection of many possible model runs and they do not cover the range of uncertainty inherent in the climate scenario simulations. Details about the A1B model run, the regional climate model ALADIN (CNRM-RM4.5, Radu et al., 2008), and the post-processing applied are described in Meißl et al. (2017). The RCP8.5 scenario is based on the GFDL CM3 global circulation model (Donner et al., 2011) and the regional climate model WRF (Michalakes et al., 2001) in an optimized version for the Alpine region (Arnold et al., 2012). The RCP8.5 data, originally a grid data set with a spatial resolution of 10 km and a temporal resolution of one day, was bias corrected by means of the quantile mapping technique (Déqué, 2007) using the gridded data set of EURO4M (Isotta et al., 2014) for precipitation and the SPARTACUS data set of the ZAMG (Hiebl and Frei, 2016) for temperature. In a second step the data was spatially localized to a 1 km × 1 km grid using the

INCA data set (Haiden et al., 2011). Radiation and relative humidity have been downscaled using a simple scaling approach in which the climatology of the simulations for the reference period is adjusted to that of the INCA data set. The applied scaling method does not modify the day to day variability, thus the physical linkages between the variables radiation, precipitation and humidity that should be reproduced by the regional climate model are conserved. For further use in the hydrological modelling, temperature was disaggregated to hourly values based on the daily maximum and minimum temperatures using three piecewise continuous cosine curves. Radiation, relative humidity and wind speed were disaggregated using the methods descripted in Debele et al. (2007). Precipitation was disaggregated using stochastic functions whose distributions were derived from 10-minute precipitation recordings at stations close to the target area (Koutsoyiannis, 2003; Goler and Formayer, 2012). The precipitation parameters considered in the statistical analysis include (i) intensity, (ii) wet period duration (number of successive time steps with precipitation), (iii) number of wet periods during the day and (iv) starting time of each wet period. The first three parameters resemble a gamma distribution and the last one a uniform distribution.

First the number of wet periods for the day was randomly chosen based on the statistics derived from the station recordings. For each wet period (continuous 1 h intervals with a non-zero rain amount) a random fraction of the daily precipitation was assigned. The starting time and duration of the wet periods were stochastically chosen based on the observational statistics. The precipitation amount was then randomly distributed over this wet period with the requirement that the sum is equal to the original one. Physically unrealistic precipitation intensities were avoided by imposing a temperature-dependent upper limit which was determined from the monthly temperature and precipitation intensity statistics of the original stations. Due to the stochastic nature of this disaggregation method, it was only applied to one grid point within the catchment area. The precipitation intensity for the remaining grid points was calculated based on this generated 1 h time series and subsequently scaled by a factor determined by the daily precipitation totals from the original climate scenario. This ensures a spatial consistency with the timing of the rainfall across the catchment.

The two climate scenarios project an increase in annual mean temperature of approximately 3.4 K until the end of the century (after bias correction and downscaling; compared to the reference period 1981–2005) in the case of A1B, and an increase of about 8.9 K until the end of the century in the case of RCP8.5 (see Fig. 2). Until 2100, annual precipitation is expected to decrease by 287 mm (A1B) or 504 mm (RCP8.5) which corresponds to a relative precipitation decrease of 18 and 29%.

In the A1B scenario, an increase in annual mean temperature by around 1.1 K until the decade 2031–2040 is expected with a rather balanced warming in summer and winter. Temperature rise will go up to 2.1 K in annual mean temperature until the 2050s, with again only little differences between winter and summer. Precipitation shows no clear trend in the first half of the 21st century, and annual precipitation remains about the same (Fig. 3). At the end of the century, a decrease in summer precipitation can be observed (around 128 mm, corresponding to 31% in the months of July and August) with no clear trend in winter precipitation. Figs. 2 and 3 show that the decadal variability of the precipitation development is much higher than the one for temperature. In the RCP8.5 scenario, an increase in annual mean temperature of 3.5 K is expected until the decade 2031–2040 with the most distinct increase of 5.3 K in October (see Fig. 2). In the middle of the century the temperature increases for all months most notably. The warming maxima at the end of the century are in August–October (approx. 9.8 K) and February–April (approx. 9.7 K). The anticipated precipitation shows a clear decreasing trend during the whole 21st century, interrupted by a wet period in the 2040ies (Fig. 3).

According to the estimation of the stakeholders the effects of climate change in the moderate A1B scenario should remain manageable. The increase in temperature results in a prolongation of the growing period up to three weeks in 2030 and water availability is sufficient. Farming and forestry benefit from the CO_2 fertilization effect. However, single dry and hot summers could become the cause of declining harvests in grassland farming, shorter mountain pasture periods and bark beetle calamities in forestry. Further, the risk of forest fire rises, but their occurrence remains rare. Tourism in summer as well as in spring and autumn is supposed to benefit from the warmer and partly steadier weather conditions, but winter tourism will suffer from a reduction of the natural snow cover period and the efforts for technical snow production will have to be intensified. The consequences of the extreme RCP8.5 scenario for the Brixental should remain manageable at least until 2030. Effects of climate change will accentuate until 2050, which especially affects farming and forestry. Even if droughts in some years reduce the harvest, farming is expected to generally benefit from higher temperatures. For forestry these conditions cause problems, as the current species composition of the forests (high share of spruce) is not suitable. Also in this scenario, winter tourism suffers from a lack of natural and technical snow. However, with the general warming traditional summer holiday destinations become too warm, so that higher Alpine areas benefit with their agreeable climate conditions.

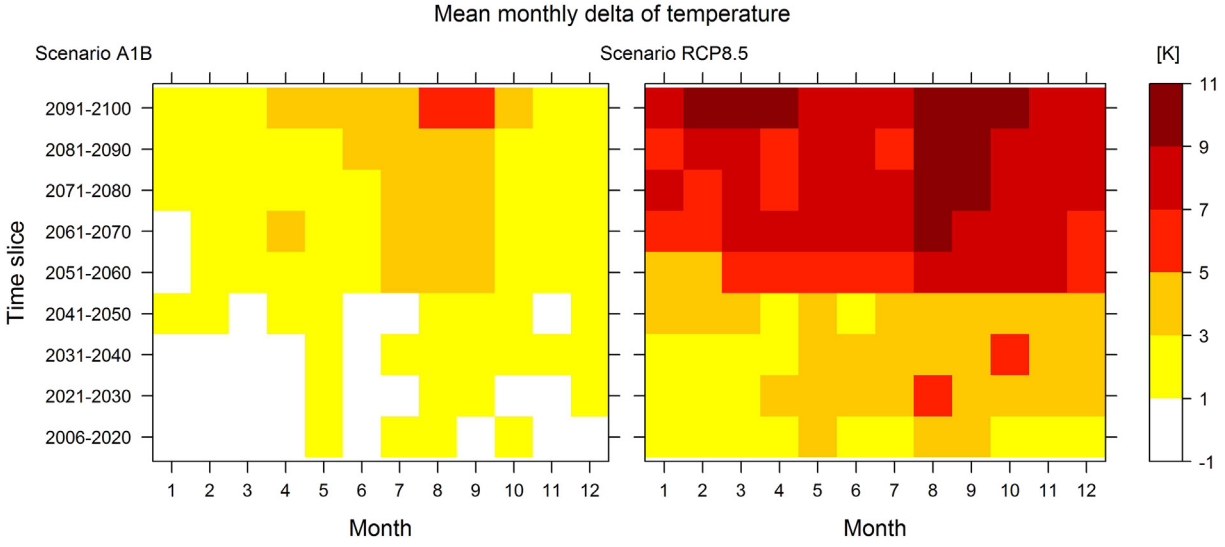

Fig. 2. Change in mean monthly temperature during the 21st century for the study region relative to the reference period 1981–2005 for the climate scenarios A1B (left) and RCP8.5 (right).

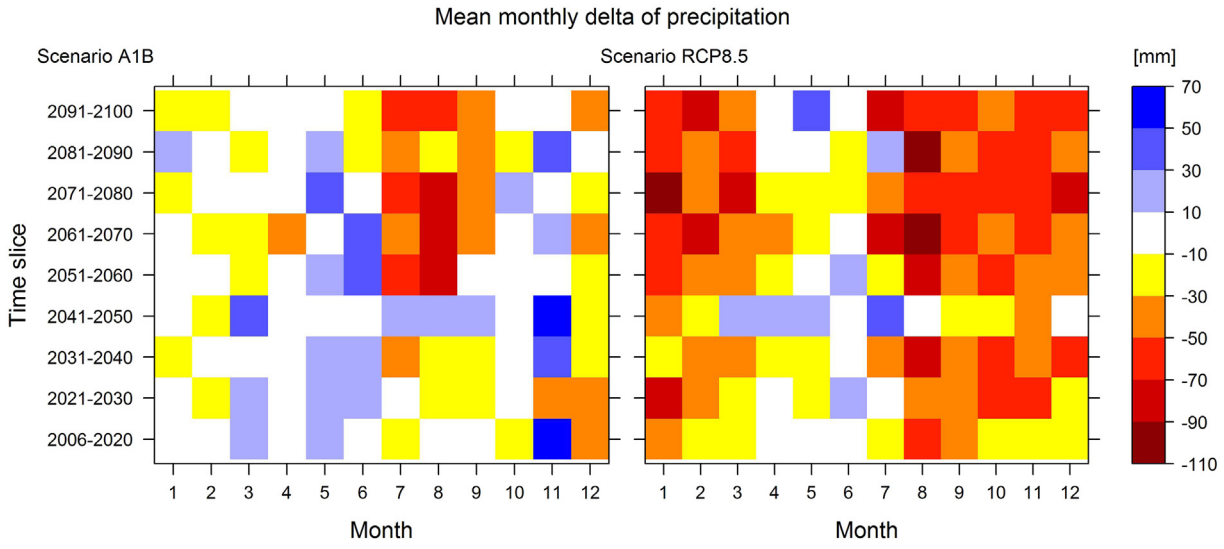

Fig. 3. Change in mean monthly precipitation during the 21st century for the study region relative to the reference period 1981–2005 for the climate scenarios A1B (left) and RCP8.5 (right).

3.2. Socio-economic scenarios

The climate scenarios were coupled with socio-economic scenarios, representing possible future developments of the local socio-economic conditions. With respect to potential future land use, it turned out that mainly the forestry system would be affected by the expected changes in the local socio-economic conditions. In agricultural land use we currently observe opposing trends. Flat areas where big machinery can be used are managed more and more intensively, while the mowing of slopes is reduced and replaced by grazing or afforestation. Similarly, the alpine pastures are gradually abandoned, or milking cows are replaced by young stock or suckler cows. Both trends result in an increase in the forest covered area.

We started with a broad review of scientific literature and public government documents; this provided an overview of the current discourse on the local climate change effects on forestry. Then, semi-structured interviews with local forest experts were conducted in order to jointly learn about actual forest management issues (like current composition and future change of tree species) and the cooperation among forest owners. A subsequent quantitative survey mostly confirmed the previous assumptions. The result of this mixed method approach provided the basis for constructing our socio-economic scenarios for which the concept of "community resilience" was applied (Wilson, 2012). This concept translates the different configurations of capitals available within a community into differing strategies, resulting in "relocalized", "glocal" or "super-globalized" communities (Fig. 4). Capital is thereby defined as the availability of environmental, economic and social resources. Depending on the combination of capitals, each of the three basic land use scenarios can have a resilient or vulnerable configuration.

3.3. Storylines of combined future land use and climate evolution

The resulting preliminary six socio-economic scenarios were merged with the A1B and RCP8.5 scenarios, resulting in 12 coupled scenarios of local land use and climate (Table 1, in the Appendix). These scenarios were discussed regarding their plausibility and consistency in a workshop with local stakeholders coming from different professional backgrounds like agriculture, forestry, hydrology, regional development and tourism. As some of the scenarios turned out to have quite

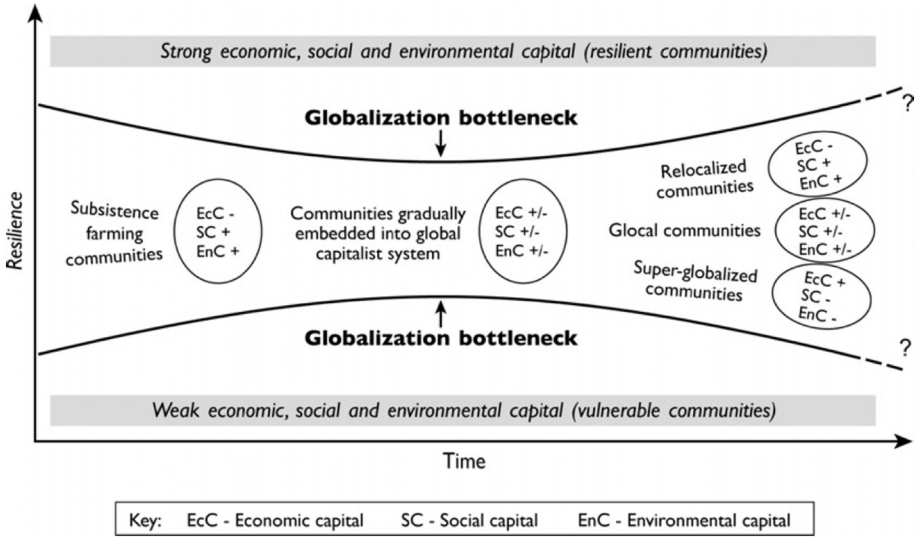
Strong economic, social and environmental capital (resilient communities)
Globalization bottleneck
?
Subsistence farming communities
EcC - SC + EnC +
Communities gradually embedded into global capitalist system
EcC +/- SC +/- EnC +/-
Relocalized communities
EcC - SC + EnC +
Glocal communities
EcC +/- SC +/- EnC +/-
Super-globalized communities
EcC + SC - EnC -
Globalization bottleneck
?
Weak economic, social and environmental capital (vulnerable communities)
Resilience
Time
Key: EcC - Economic capital SC - Social capital EnC - Environmental capital

Fig. 4. Types of communities and changing community resilience over time. From Wilson (2012, p. 1224).

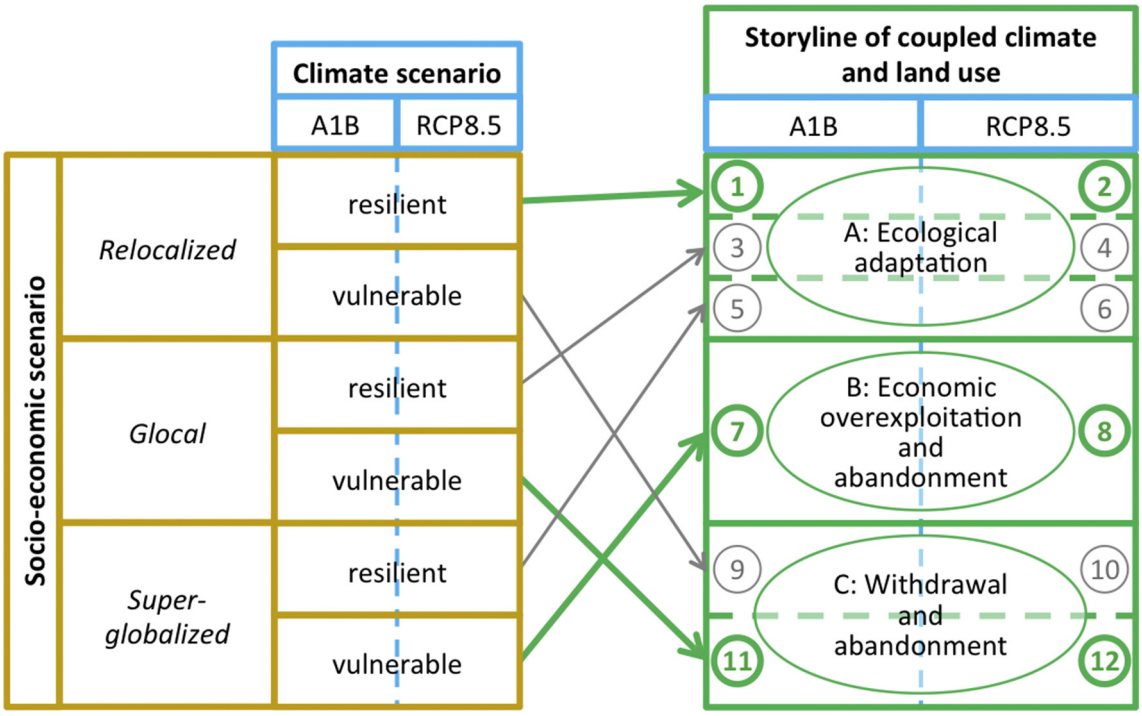

Fig. 5. Classification of the storylines of coupled scenarios of local land use and climate. The bold arrows and numbers indicate those storylines chosen as input to the hydrological modelling.

similar consequences we distinguished three general distinct evolutions of forest management: A) ecological adaptation, B) economical overexploitation and abandonment and C) withdrawal and abandonment (Fig. 5). In combination with one of the two local climate futures (according to A1B and RCP8.5, respectively), these evolutions are called "storylines" in the following. Each of the 12 coupled scenarios of local land use and climate (left side in the figure) can be assigned to one of the three storylines (arrows to the right side in the figure). In order to cope with the computational restrictions related to the later hydrological scenario simulations, for each storyline a socio-economic/climate scenario representative was selected for the modelling, ensuring that all three types of socio-economic scenario (relocalized, glocal, super-globalized) and both climate scenarios are used.

The three storylines are described as follows, based on distinct evolutions of forest management (Table 1 in the Appendix):

A) Ecological adaptation: In forest management the political guidelines are consequently applied. The forest cover is dominated by an ecological, locally adapted mixed cultivation with a harmonious age structure. Thus, the forest is generally resilient towards natural hazards and simultaneously fulfils its different functions. Marginal land on steep slopes is reforestated, alpine pastures are used for cattle and sheep as today. Natural reforestation is partly possible due to extensification, a process that is already ongoing now.

B) Economical overexploitation and abandonment: Forest management focuses on increase in efficiency, cost reduction and short term results. Nevertheless, legal regulations are respected and new, adapted species are reforested (e.g. Douglas firs). After a short intensive phase of forestry use and overexploitation, the forest managers lose their economic interest due to decreasing profit. Agricultural activities are concentrated on few large farms. Marginal land is reforestated, alpine pastures are mainly abandoned.

C) Withdrawal and abandonment: The forest cultivation is generally decreasing. With the withdrawal the forest becomes vulnerable against natural hazards. Alpine pastures are nearly completely abandoned.

The qualitative information of the storylines was translated into rules executable by raster operations with a GIS (Geographical Information System) with the help of two local forestry experts. These rules, e.g. "grassland (hay meadows) extents remain unchanged" (storyline A) or "grassland with a slope > 35% is abandoned and successively reforested with the neighboring forest type" (storylines B and C) enabled the production of a time series of land use maps as required by the hydrological modelling (Fig. 6). For each storyline a series of 9 land use maps with a 10 year increment was created (2020−2100). These maps (as well as the modelling results themselves) were again evaluated and checked for plausibility by the local stakeholders.

The stakeholder process was undertaken as a transdisciplinary method to systematically translate local knowledge into suitable data (following Bay-Larsen and Hovelsrud, 2017). In our case the local knowledge allowed to further deepen and validate the initially purely research-based storylines (Walz et al., 2007). The inclusion of local knowledge by participative approaches further contributed to increase the legitimacy of the socio-economic scenarios (Nilsson et al., 2017). Participatory development made the storylines more relevant to the stakeholder needs and priorities and, finally, encourages adaption to future changes among the stakeholders (Reed et al., 2013; Schermer et al., in review). Moreover, the process of participative scenario generation fostered the dialogue among experts, decision-makers and stakeholders, and supported to bridge the gaps between the latter and the research community (Stotten et al., 2018; Mallampalli et al., 2016).

In a second stakeholder workshop the results of the hydrological modelling were discussed with the same local stakeholder group as in the first workshop. Finally, it was jointly considered if and how the project results could be utilized to support and contribute to the local and regional development strategies.

3.4. The hydrological model WaSiM

3.4.1. Model description

For hydrological modelling of streamflow of the Brixentaler Ache we used the physically based model WaSiM (Water Balance Simulation Model) (Schulla, 1997, 2015) which describes the water fluxes on land surfaces, including the subsystems of vegetation and soil and the lateral fluxes along the river to the gauge at the outlet of the catchment. WaSiM has already been used successfully in a wide range of applications

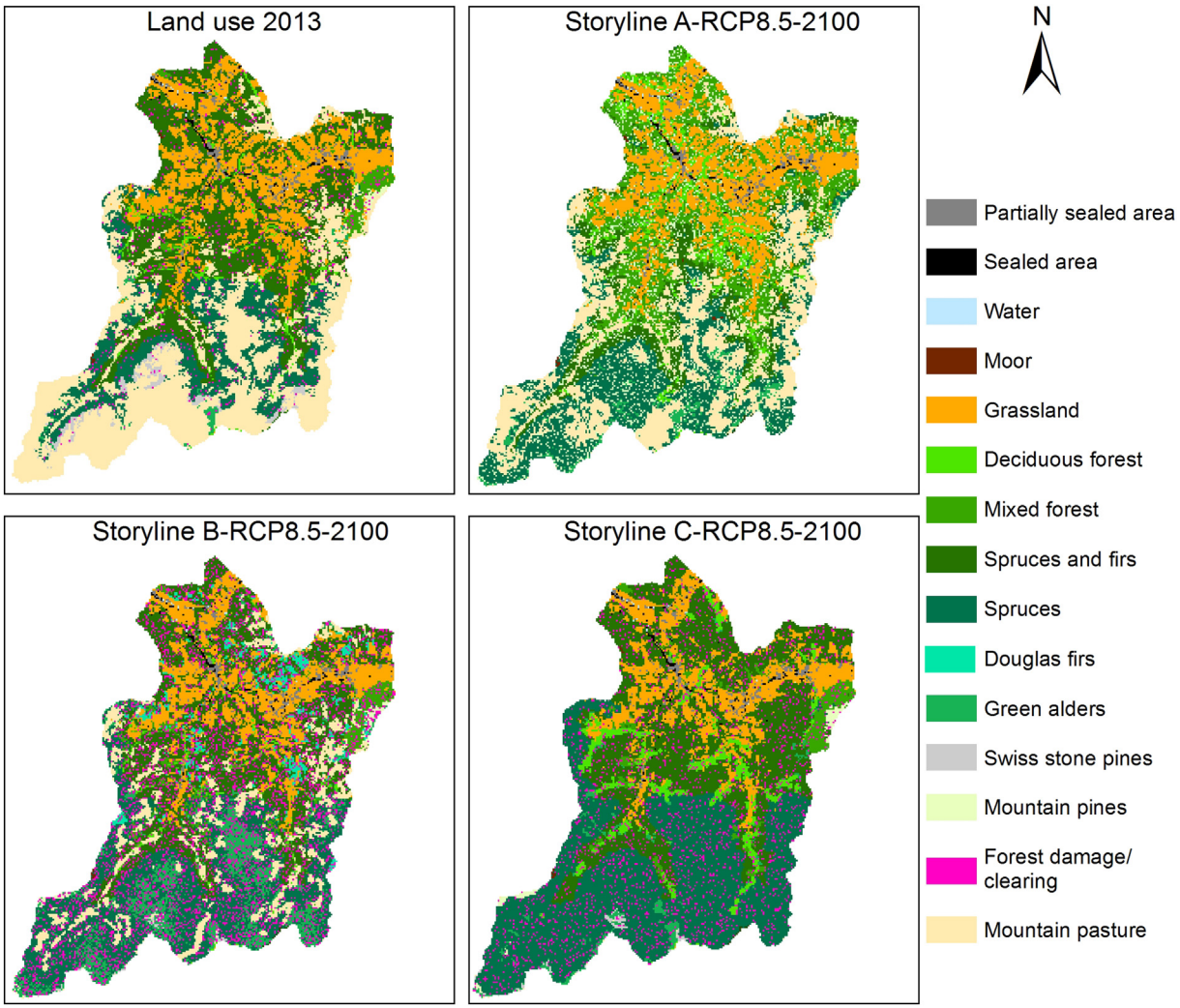

Fig. 6. Land use maps for current (2013) and future (2100) situation for the storylines A-RCP8.5, B-RCP8.5 and C-RCP8.5. The state as of 2013 is derived from the data set of the Federal Province of Tyrol (Federal Province of Tyrol, 2012) and the Schiechtl/Stern Forest map (Federal Province of Tyrol, 2009).

(e.g., Bormann et al., 2007; Cullmann et al., 2006; Kraller et al., 2012; Kunstmann and Stadler, 2005; Natkhin et al., 2012; Niehoff et al., 2002; Schulla, 1997; Warscher et al., 2013). The hydrological processes are computed on a regular grid and at hourly or daily time steps. Rain interception is computed using a bucket approach, capable of representing layered vegetation. This allows for computing interception in the canopy, and also in the understory beneath the trees. All intercepted water is subject to evaporation or throughfall. Evapotranspiration is calculated using the Penman-Monteith method (Monteith, 1965). Therefore, parameters for major plant characteristics are input to the model, distributed to a seasonal course (see Section 3.4.2). Infiltration, computed according to Green and Ampt (1911), is coupled with a complex numerical scheme based on the Richards equation (Richards, 1931) used for closing the soil water balance. The soil is represented by a one-dimensional vertical discretization of soil layers. The runoff components are calculated by balancing the soil moisture water content with infiltration, actual evapotranspiration and saturation. Surface runoff is the water not infiltrating the soil, and interflow is a fast runoff component originating from the soil. A two-dimensional groundwater model can be coupled to the numerical soil water scheme. Alternatively, a linear reservoir model for computing baseflow can be used, representing the outflow from the saturated layers. This simpler linear storage model proves helpful in cases where the required data is not available, as in mountainous catchments like the study site. Finally, runoff routing is computed using the Manning-Strickler equation (Strickler, 1923; Schulla, 2015).

Recently, WaSiM has been extended for specific snow processes, e.g. lateral snow transport (Warscher et al., 2013), and a layered snow model as well as heat transport in the soil and the snowpack for representing permafrost (after Daanen and Nieber, 2009). The processes at the snow surface can now be computed by means of the energy balance approach (Warscher et al., 2013). In the newest model version, a snow interception storage has been introduced that accounts for intermediate snow storage inside a forest canopy (Förster et al., 2018). Including the snow-canopy interaction in WaSiM considerably improves the performance of streamflow simulations in catchments with significant forest cover and snowfall during winter (Förster et al., 2018).

The new WaSiM version is specifically designed for application in high mountain regions. An additional advantage is the possibility of running the model with arbitrary spatial and temporal resolution. This allows for better considering the physical processes of snow melt which are largely controlled by the daily course of global radiation.

3.4.2. Parametrization of evapotranspiration

A reliable representation of evapotranspiration (ET) is crucial in hydrological modelling since changes in land use (and hence, changes in vegetation) have major impacts on ET. In principle, WaSiM allows for an arbitrary number of land use classes that are linked to a land use map via unique class IDs. For each land use type, a comprehensive set of parameters has to be defined: albedo, canopy resistance, leaf area index (LAI), vegetation cover fraction (VCF), and root depth. Based on

a detailed literature review, we developed a detailed parameterization for all land use classes in our study region (see Table 3 in the Appendix). While most settings could be adopted from the existing WaSiM configuration (Schulla, 2015), the following has been considered in addition:

- Breuer et al. (2003) provide most of the required parameters for many species prevailing in our study area. In their study, canopy resistance values for tree species are taken from Körner et al. (1979). Additional parameters were taken from Markart et al. (2012) and Federer et al. (1996).
- For the lacking parameters for mountain pine we adopted values found for Scots pine. Douglas fir was assumed to have a slightly higher albedo than spruce (based on personal estimation of the stakeholders), and the values of root depth have been increased – also for firs – after Nadezhdina et al. (2014). Since most parameter values (except for canopy resistance) were unknown for Swiss stone pine, we adopted the respective values found for Scots pine.
- Both winter and summer values listed of each parameter in Table 3 (in the Appendix) are utilized to construct a diurnal course for each land use class. The common method to construct annual cycles for each parameter in WaSiM is the "VariableDayCount" approach (Schulla, 2015). Since no validation data that describe changes in phenological characteristics as response to climate is available – neither for our land use classes nor for the study area – we applied a static annual cycle. A dynamic approach that enables to adapt the vegetation season to changing climate conditions would require either appropriate phenological observations, or a fully coupled plant growth model.

A direct and spatially distributed validation of the WaSiM ET simulations is not possible; both point-scale observations (e.g., eddy flux method) as well as catchment-scale validation data (e.g., from remote sensing) are not available in the catchment. The latter also relies on ET models which are forced by radiances. Even though it is possible to calibrate the ET parameters – at least for a small number of classes – using the Penman-Monteith approach (Birkinshaw et al., 2014; Bie et al., 2015), vegetation parameters are mostly estimated a priori, because (i) adequate validation data is lacking and (ii) the degree of freedom in calibration would be increased since several parameters for numerous land use classes are relevant to simulate ET in a realistic way. Still, the Penman-Monteith approach in WaSiM with its prescribed parameter sets for forests is scenario-capable if long-term changes of the water balance are analyzed (Beckers et al., 2009a, 2009b; Adams et al., 2010). ET validation is enabled through model calibration by minimizing the volume bias (i.e., the difference between observed and modelled streamflow). Since ET is the remainder term in the long-term water balance (and proper precipitation data is available), there is evidence that ET is modelled in a reliable way. Calibration and validation of the model are described in section 3.4.4.

3.4.3. Snow-canopy interaction

As we want to investigate the hydrological impacts of changing land use, both summer and winter interception processes have to be considered by the hydrological model applied here. Snow-canopy interaction can significantly affect the streamflow signal, and this particularly holds true for a catchment in the subalpine elevation zone where the winter season is characterized by several intermittent snow accumulation and melt periods (Förster et al., 2018). If the snow surface energy balance is to be calculated beneath the trees (i.e., no melt coefficient is calibrated), an explicit consideration of the micrometeorological conditions at the surface of the ground snow cover during the winter season is required (Strasser and Etchevers, 2005).

Hence, in our study we apply the new WaSiM snow-canopy interaction model extension by Förster et al. (2018) featuring (i) snow interception and (ii) modified micro-meteorological conditions under coniferous forests. The used snow-canopy interaction model is based on the work of Liston and Elder (2006) and has already been integrated in several snow and hydrological models, differing in some of the used parameterizations and level of detail (Förster et al., 2018; Strasser et al., 2011). With the new snow-canopy interaction model extension, WaSiM can be used for simulating the hydrological fluxes inside canopy stands, a cogent research issue (Tappeiner et al., 2008; Tenhunen et al., 2009; Varhola et al., 2010; Mahat et al., 2013; Leitinger et al., 2015; Dickerson-Lange et al., 2017; Schirpke et al., 2017).

3.4.4. WaSiM model calibration and evaluation

The model was calibrated using the lexicographic calibration scheme introduced by Gelleszun et al. (2017). This process-oriented approach optimizes parameters which are linked to specific processes in individual calibration steps. For this study, we performed two calibration steps in sequence: The first step includes parameters of the soil model (flow density and recession of saturated hydraulic conductivity with soil depth). These parameters govern the dynamics of interflow. Subsequently the parameters of the linear storage groundwater recession model were calibrated (scaling parameter and recession constant). The second calibration step involves a minimization of the Root Mean Square Error (RMSE) computed for the lowermost 35% of the modelled and observed flow duration curve. This subdivision into single calibration steps allows for calibrating the model automatically with an acceptable number of iterations (100 to 150) while considering different objective functions and acknowledging physically meaningful and transferable parameter sets (Gelleszun et al., 2017). The resulting performance measures – computed for both the calibration and the validation period – are compiled in Table 2 for the Bruckhäusl gauging station (see Appendix A). A spin-up period of one year was considered for the simulations (i.e., even though the calibration covers 2008–2012, the simulations were initialized in 2007).

The model skill achieved suggests that the model reliably matches observed states for both the calibration and the validation period. The Nash-Sutcliffe model efficiency (Nash and Sutcliffe, 1970) is well above 0.5, indicating an acceptable model performance. The absolute values of the percentage BIAS (PBIAS, a relative measure of difference between modelled and observed streamflow) are around 5% which is regarded as a good representation of the multi-annual water balance. In order to relate the RMSE to the dynamics of the time series, the ratio of the RMSE to the standard deviation of observed data (RSR) is computed. The achieved RSR values clearly below one and close to 0.5 are satisfying. Moreover, values of Pearson correlation higher than 0.8 indicate a skillful phase coincidence between the modelled and observed time series. Since the performance measures are similar in both periods, it is concluded that the model tracks the observed time series well, given that only four parameters are adjusted (Fig. 7 (a) and (b)).

Due to the limited availability of highly resolved data for forcing the model (hourly meteorological input, see Section 2) and corresponding data for evaluating the model (streamflow data), the temporal coverage of the calibration and validation periods is short given that the model is designed for long-term scenario applications. Still, the calibration period covers a reasonable variety of different years in terms of anomalies of temperature and precipitation, respectively. It is therefore assumed that this period reflects a sufficient variability of conditions even though it only covers 4 years. In order to judge how the model is capable of correctly representing the water balance at longer time scales, the WaSiM runs forced by the historical regional climate model data were analyzed. Since the meteorological forcing provided by the regional climate models statistically represents the climate of multi-decadal periods, it is possible to compare streamflow statistics computed for WaSiM runs forced by the two regional climate models to the ones forced by corresponding observations from the same period. Fig. 7 (c) provides flow duration curves (FDCs) of observed and modelled streamflow

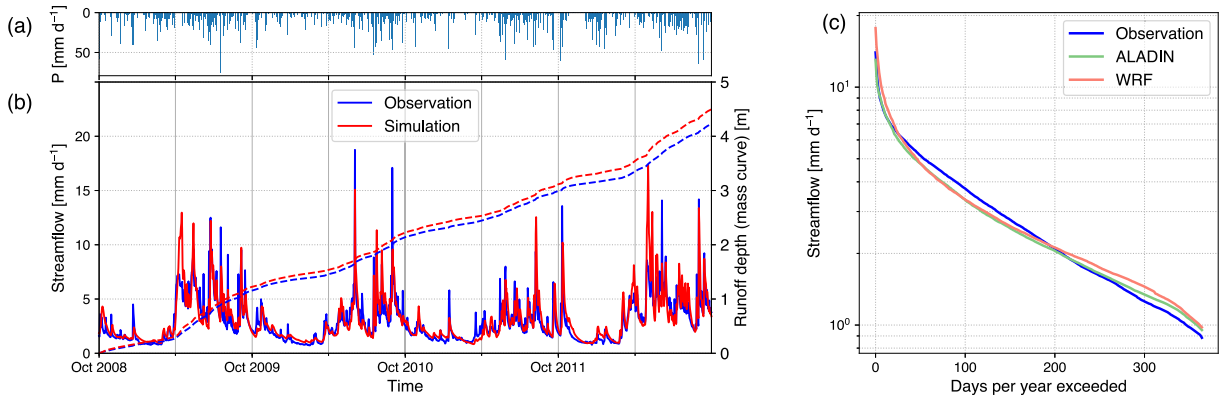

Fig. 7. (a) Areal precipitation (P) in the calibration period. (b) Observed and modelled streamflow in the calibration period. The dashed lines represent the mass curves computed for the streamflow time series. (c) Flow duration curves (FDCs) for past climate conditions obtained by forcing WaSiM with the climate model data ("ALADIN" and "WRF") of the period 1981–2005. A corresponding (in terms of temporal coverage) observed FDC is plotted for reasons of comparability.

constructed for the period 1981–2005. Since the FDCs constructed for the WaSiM runs forced by the climate models match the observed FDC very well, it can be noted that (i) the bias correction applied to the raw data from the regional climate models is suitable for representing hydrological processes and (ii) the WaSiM parameterization achieved by model calibration is also suitable for long-term scenario analyses. The small differences in terms of mean annual streamflow suggest that both the bias correction and the hydrological model are suitable for reconstructing past hydrological conditions.

4. Results and discussion

4.1. Land use change resulting of the storylines of combined future land use and climate evolution

In the modelling of the water balance, the land use data is updated every ten years with a new map of its distribution in the catchment. The date for the replacement is always October 1, since in autumn the hydrological storages are assumed to be mostly empty or at least below average, and hence the discontinuity caused by the map replacement is minimal. We assume that the remaining effect can be neglected in the interpretation of the results given that the number of changes is small compared to the number of years used for computing averages (10 or 30 years, described in the next section).

Fig. 8 shows the land use changes resulting from the storylines of coupled scenarios of local land use and climate. The areas used for grassland management in the valley floors do not change in storyline A and slightly decrease in B and C. There it is assumed that meadows steeper than 35% which cannot be cultivated by machines are abandoned and then mainly naturally reforested. Due to the fact that in A forest management supports a return to the original diversity of the species composition, deciduous and mixed forests expand in the first half of the century at the expense of coniferous forests. While in storyline A only a marginal number of areas of the mountain pastures is abandoned, their reduction is stronger in B and complete in C. Abandoned mountain pastures are at first overgrown with green alders which are gradually substituted by coniferous trees. Thus, the development of areas with green alders and coniferous forests strongly depends on the mountain pasture areas. Differences between A1B and RCP8.5 climate scenarios mainly become obvious as larger proportions of areas deforested by clear cutting, windfall and bark beetle damages. In case of storyline A, the differences between the underlying assumptions of A1B and RCP8.5 climate is small in terms of the expansion of deciduous and mixed trees, since we assume that mountain pastures are still cultivated regardless the different evolutions of the tree line. Douglas firs are only used in B showing the intensification strategies. Settlement areas always remain constant (2.3% of the catchment area).

4.2. Water balance

4.2.1. Mean annual streamflow in past and future periods

In the following, the results of the hydrological simulations with WaSiM using the developed combined future land use and climate scenarios and their effects on the water balance of the Brixental are discussed. All simulations were performed as transient model runs covering the period 1981–2100 for each storyline. Our detailed evaluations were focused on both the historical period 1981–2005 and the future periods 2005–2035, 2035–2065, and 2070–2100. The used storylines A, B and C comprise the forest management practices and the climate scenarios A1B and RCP8.5 in all possible six combinations as described in the previous sections. In addition, we applied the model for the two climate scenarios with constant historical land use conditions, denoted in the following as "Baseline". According to the availability of the data, the "Baseline" land use distribution corresponds with the status in 2013. In this way we can distinguish between the effects of a changing climate solely and the ones of a changing land use combined with climate change.

Starting from the results illustrated in Fig. 7 (c) which demonstrate the capabilities of the model to simulate past hydrological conditions when forced by bias-corrected regional climate model data, we analyze the long-term simulations of the storylines using mean annual streamflow. This analysis provides a first idea of how the water balance changes on average according to our simulations using the storylines. The usage of mean annual streamflow as starting point for the analyses enables a simple comparison with corresponding values for past conditions; it is available in many cases even in the absence of observed time series with high temporal resolution. Moreover, changes in mean annual streamflow provide a first guess for judging changes in water availability since it is easily comparable to other sites. Fig. 9 shows the mean annual streamflow computed for the storylines with their different underlying climate forcing. The blue bar indicates the streamflow observed at the Bruckhäusl gauging station. On average, the mean annual streamflow amounts to 1092 mm/yr there.

In the period 1981–2005 all storylines share the same land use map which was a basic assumption in the study design and attributable to the lack of a consistent time series of snapshots of past spatial land use distributions. This explains why each storyline yields the same mean annual streamflow for a given climate scenario. When compared to the corresponding observed mean annual streamflow, the differences are small. If WaSiM is forced with the A1B data for the historical period, the mean annual streamflow is subject to a bias of −48 mm/yr (−4%). Similarly, the RCP8.5-based simulations for the past even indicate smaller differences: the bias is +10 mm/yr (+1%). The differences are found to be small given that there are uncertainties arising from several previous calculation steps including the assumption of stationarity in

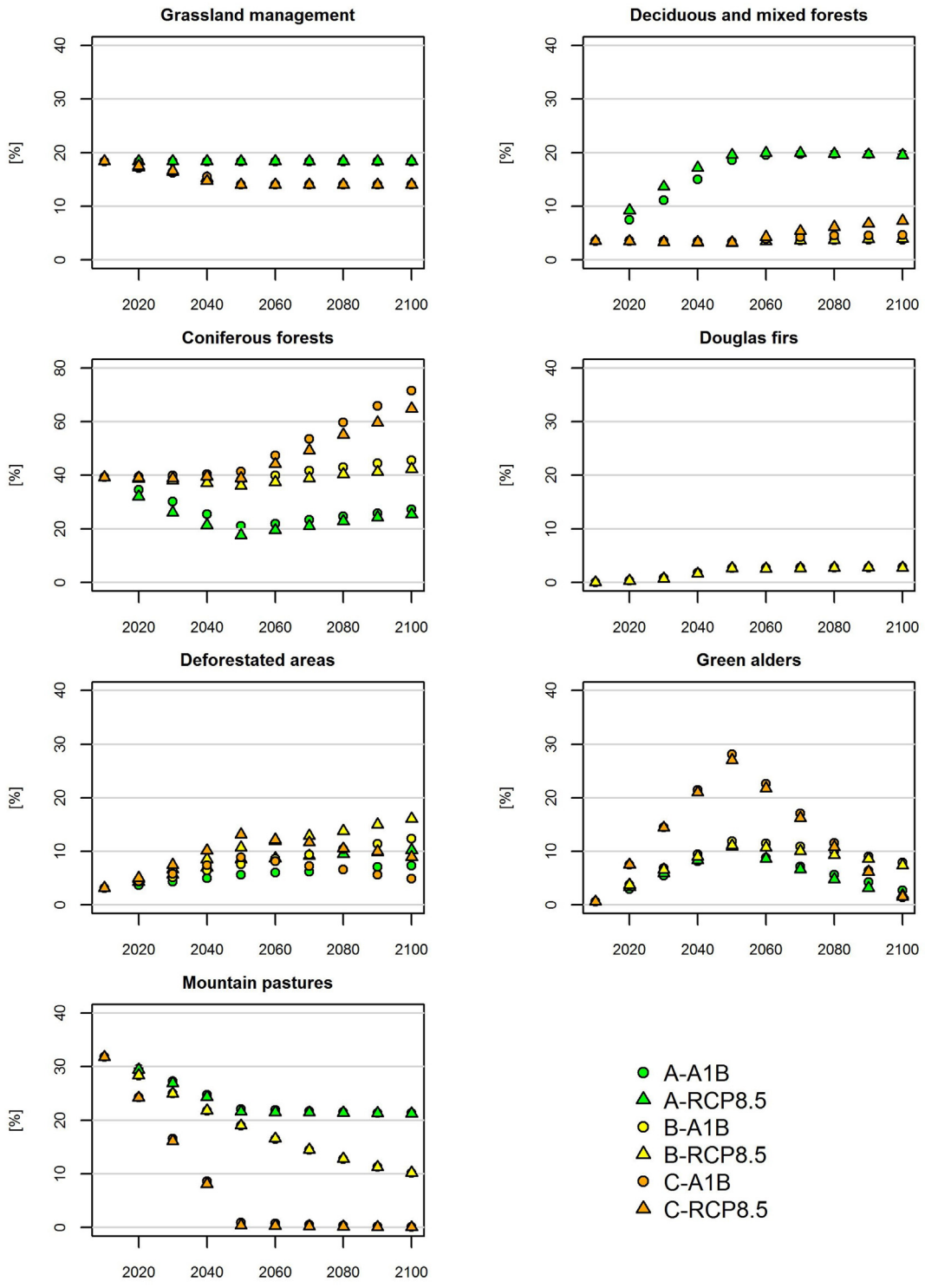

Fig. 8. Changes of land use proportions in the Brixental for the developed storylines.

land use in the past, involving climate models at global and regional scales, downscaling, and hydrological simulations. Still, it has to be kept in mind that such analysis of the water balance is only valid in terms of aggregated measures like, e.g., FDCs or mean values, since the climate models represent the climate only in terms of statistical features, rather than reconstructing it on an actually observed day-by-day evolution of weather.

An important aspect in the interpretation of the results is the separation of the effects on the mean water balance components originating in climate change on the one hand, and in combined climate change with corresponding land use development on the other. The evolution of frequencies and the extent of extreme events are not interpreted here, however, since hydrological extremes were not explicitly addressed for calibrating the model. Generally, it can be expected, that – without consideration of a changing land use – an increase in the mean summer temperatures (see Fig. 2) and a reduction of precipitation in this season (see Fig. 3) will lead to an increase in evapotranspiration, and finally, to a decrease in streamflow. As a consequence of this, less water is available for anthropogenic demands such as hydropower generation, irrigation or other uses. In Fig. 9, this climate-change-only related effect is

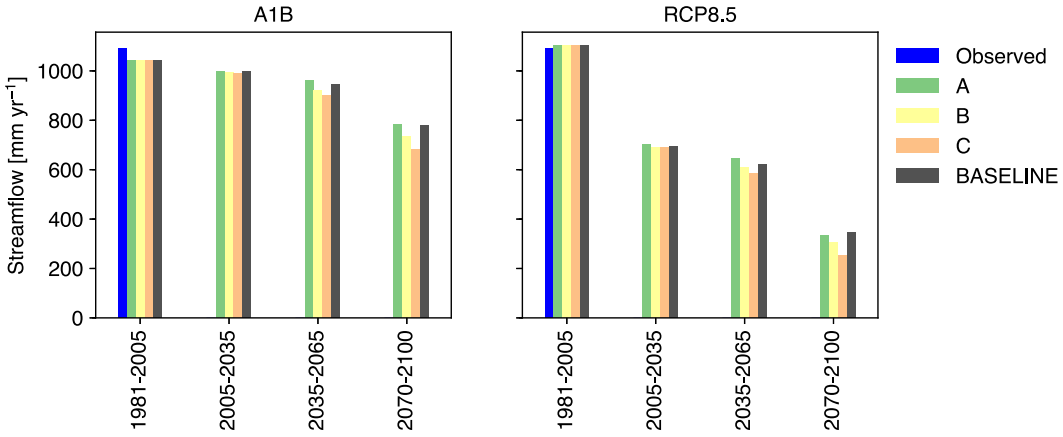

Fig. 9. Mean annual streamflow at the gauge Bruckhäusl (525 m a.s.l., 322 km^2) for the storylines A, B and C with A1B and RCP8.5 climatic conditions until 2100.

visualized with the "Baseline" simulation for the A1B and RCP8.5 scenarios, respectively (gray bars in the figure): When considering the climate-only effect on the water balance, streamflow decreases by 46 mm/yr (−4%, 2005–2035), 99 mm/yr (−9%, 2035–2065), and 263 mm/yr (−25%, 2070–2100) in the A1B scenario. The corresponding values for RCP8.5 are 406 mm/yr (−37%, 2005–2035), 479 mm/yr (−43%, 2035–2065), and 756 mm/yr (−69%, 2070–2100).

Besides climate, the model also computed changes in streamflow as response to spatio-temporal changes in land use: In A1B and for the period 2070–2100 the decease of mean annual streamflow for storyline A is 258 mm/yr (−25%), for B it is 307 mm/yr (−29%) and for C it is 362 mm/yr (−35%) compared to the reference period 1981–2005 (left in Fig. 9). In RCP8.5 the respective reduction in the same period is significantly stronger, namely 767 mm/yr or − 70% (A), 795 mm/yr or − 72% (B) and 849 mm/yr or − 77% (C) (right in Fig. 9). Hence, the modified land use amplifies the effect of climate change with respect to the reduction of the amount of water available in the stream. The decrease in streamflow in A1B is moderate until the mid of the century, and it intensifies after that. Contrary to that, in RCP8.5 the decrease starts clearly in the early century, continues moderately during the period 2005–2035 until 2035–2065, and again accelerates until 2070–2100.

The effect on streamflow induced by a change in land use is significantly smaller than the one induced by a changing climate. At the end of the simulation period (2070–2100), the effect of the changed land use in the catchment (see Fig. 8) is a reduction of streamflow – computed as absolute difference to the "Baseline" simulation using the same climate forcing – of −4 mm/yr (A), −45 mm/yr (B) and − 99 mm/yr (C) in A1B, or −11 mm/yr (A), −39 mm/yr (B) and −92 mm/yr (C) in RCP8.5, respectively. Nevertheless, even being significantly smaller, the effect on streamflow caused by changing land use is important since it intensifies the decrease in streamflow water availability as a response to climate change. The extent of this effect is mainly depending on the fraction of the forested area which can become overgrown by withdrawal of previously cultivated areas; this has already been explicitly pointed out in earlier simulation experiments (e.g., Zierl and Bugmann, 2005; Köplin et al., 2013). Furthermore, it is interesting that the absolute magnitude of the land use induced change of the runoff signal is more or less independent from climate. At the relative scale, the effect is hence larger in the moderate climate future of the A1B scenario. Indeed, for storylines B and C the effect in absolute numbers is slightly smaller in RCP8.5 than in A1B. This can be explained with the generally smaller amount of water available to plants in RCP8.5.

4.2.2. Shifts in streamflow seasonality

In order to support the last finding with data aggregated in higher temporal resolution, we now compare the mean seasonal streamflow regime derived for multi-decadal periods. Fig. 10 shows the mean monthly streamflow for the different storylines. From the upper left panel which refers to past conditions (i.e. 1981–2005), we can deduce that the seasonal patterns computed with WaSiM for observed and modelled data coincide well. As already mentioned, in this period no difference among the storylines is prescribed by the model in terms of land use. Differences between the simulation and the observations are obvious when considering streamflow for June and October. For the A1B data forcing these differences are slightly smaller than those computed for the RCP8.5 data forcing. However, the previous findings that the model chain (downscaling and hydrological model) is generally capable of reconstructing past hydrological conditions are still supported.

The comparison among the different periods of time reveals how climate and land use affect streamflow in the simulations. Even in the first future period (2005–2035) a remarkable difference in streamflow regime, attributable to the different climate forcing, is obvious. In RCP8.5 climate conditions, mean monthly streamflow in some months is on average >50 mm/month smaller than in the corresponding A1B simulations. This is in line with the results achieved in the analyses which involved mean annual streamflow only (Fig. 9). From the monthly means, seasonal changes become obvious as well.

In this first future period (2005–2035), the regimes significantly drift apart from each other. Whereas conditions in A1B still are similar to the ones in the historical period (to be compared to the simulated curve for 1981–2005), the course of the mean monthly streamflow in RCP8.5 already undergoes a remarkable reduction in water volume, and the snowmelt maximum in May is significantly reduced. From the period 2035–2065 onwards the effects of land use change become visible apart from those caused by climate change: mainly in the A1B future, which now leads to reduced streamflow as well, a further reduction in the remaining streamflow is generated by the modified vegetation conditions, as they would be realized in storylines A, B and C (increasing effect in this order). The hydrological process chain thereby is: increasing forest area in the withdrawn former mountain pasture regions leads to amplified evapotranspiration, where the interception processes all over the year play a role, too. For the last of the future periods (2070–2100) the initiated trend in the simulations further increases. In A1B the reduction in streamflow is significant, and land use change leads to a strong spread of the curves. Nevertheless, snowmelt still is the cause for the maximum in spring. However, in RCP8.5, where the fraction of snowfall in precipitation is so small that the summer rainfall causes a streamflow maximum in July. The drastic reduction of streamflow is further amplified by the forest management practices assumed in the storylines (again with increasing effect in the order A, B and C).

4.2.3. Inter-decadal and seasonal variations in water balance components

While the previous discussions focused on long-term averages of mean annual and mean monthly streamflow only, this section provides

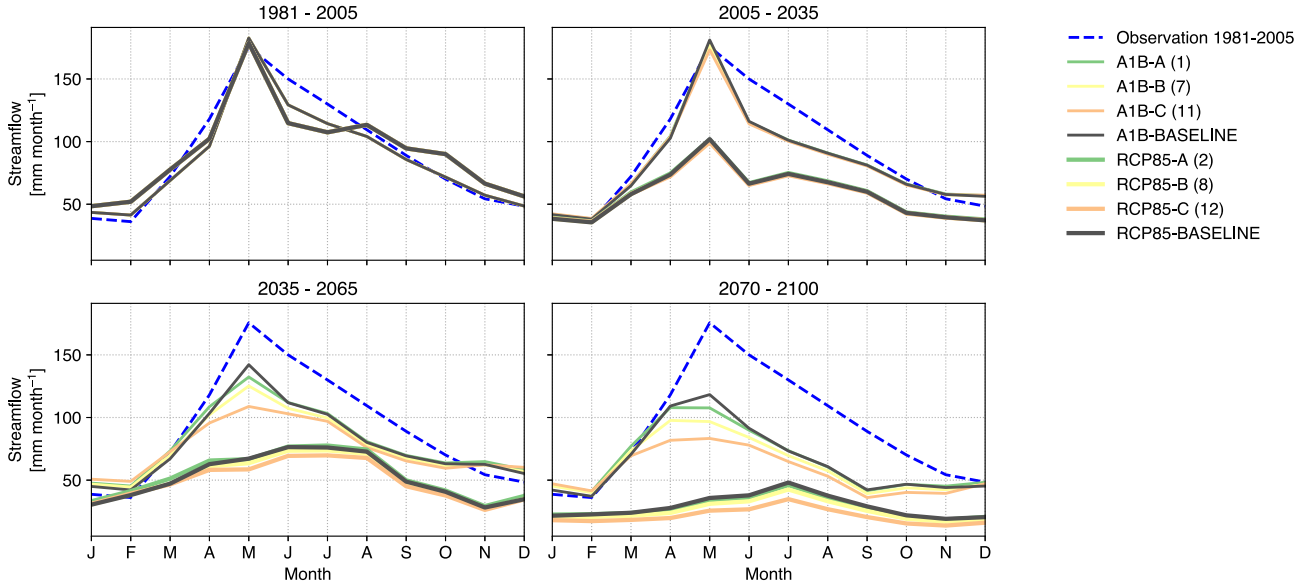

Fig. 10. Mean seasonal streamflow regime for the gauge Bruckhäusl (525 m a.s.l., 322 km^2) for the storylines A, B and C with A1B and RCP8.5 climatic conditions until 2100. The numbers in parentheses refer to the storylines in Fig. 5.

further details of the changes in seasonality and its inter-decadal variation. We also look on other water balance components. As a supplement to the long-term averages of monthly streamflow (Fig. 10), the model results for single decades in the A1B and RCP8.5 climate scenarios until 2100 for the Bruckhäusl gauging station are shown in Fig. 11. This level plot shows changes in streamflow relative to the period 1981–2005 in terms of seasonal variability along the abscissa and inter-decadal variability along the ordinate, the latter illustrating the longer-term variability in the forcing data. According to the simulations forced by the A1B climate scenario, a slight increase in streamflow in the winter months becomes obvious (blue colors in the left panel), which can be explained by the seasonal shift of precipitation. For the summer months, in contrast, the reduction in mean monthly streamflow is significant (yellow and orange colors in the left panel), with highest magnitude in May. Here the decreasing proportion of snowfall in precipitation is the reason for the respective reduction of the streamflow maximum in May. In terms of inter-decadal variability, Fig. 11 shows that the decrease in streamflow intensifies with time. In both climate scenarios, streamflow decreases towards the end of the 21st century, this effect being stronger in the RCP8.5 scenario (red colors in the right panel). In this context it is noticeable that during the 2040ies precipitation is generally higher than before and afterwards, an effect produced by both climate models used here simultaneously (see also Fig. 3). Apart from the wet 2040ies, in RCP8.5 mainly the clear decrease in mean monthly streamflow during the summer months is obvious. The maximum rate of change occurs in May because of the snowmelt effect mentioned before. Regarding the differences among the storylines, the highest decrease in mean monthly streamflow thereby amounts to approximately 160 mm (RCP8.5, 2061–2070 and 2071–2080, storyline C, in May).

The resulting effect of increasing forest area fraction on streamflow now shall be differentiated for the storylines of future development in the Brixental. Fig. 12 shows the mean monthly evapotranspiration for the simulated A1B and RCP8.5 climate scenarios in steps of 10 years. The reference for the calculation of the differences is 1981–2005. In "Baseline" the land use is the same as in this historical period. In storylines A, B and C the respective forest management practices are underlying. By these means, it will again be possible to distinguish between the effects of a changing climate only (with steady-state land

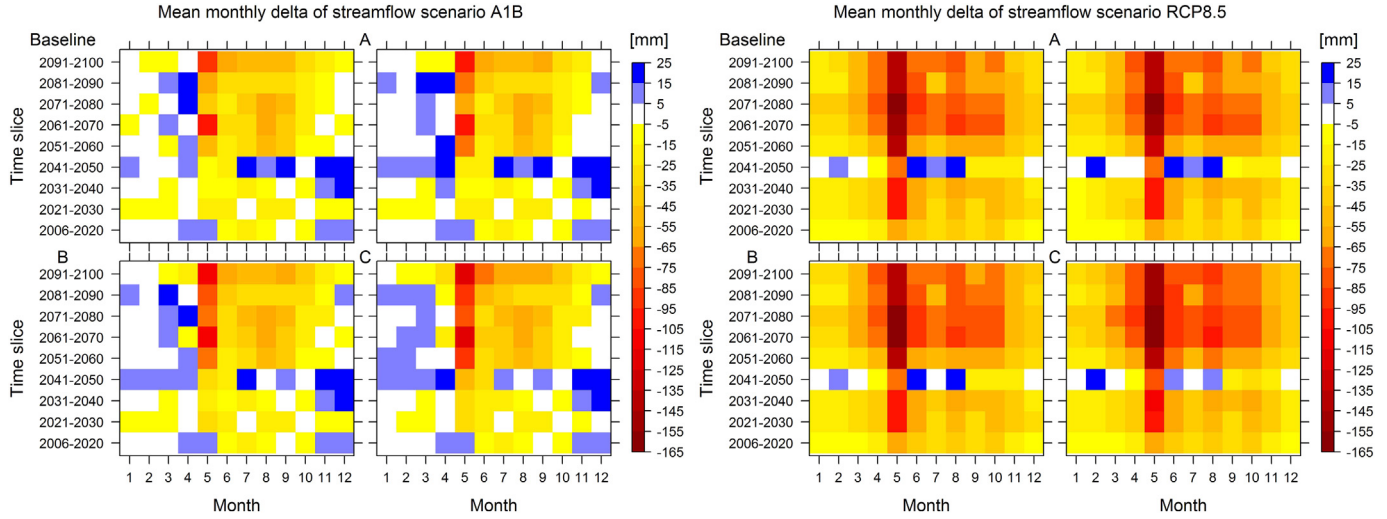

Fig. 11. Mean monthly delta of streamflow (difference to the reference period 1981–2005) for current land use ("Baseline"), as well as for storylines A, B and C with A1B (left) and RCP8.5 (right) climate scenario conditions.

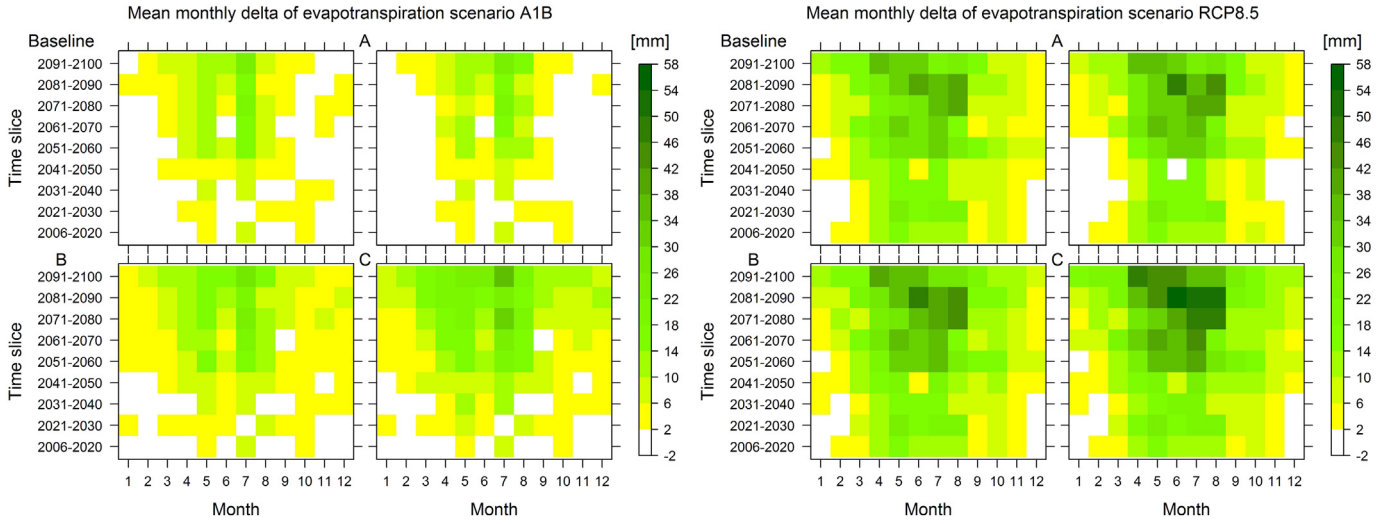

Fig. 12. Mean monthly delta of evapotranspiration (difference to the reference period 1981–2005) for current land use ("Baseline"), as well as for storylines A, B and C with A1B (left) and RCP8.5 (right) climate scenario conditions.

use conditions – "Baseline"), and the ones of a combined changing land use and climate change. When land use is unchanged (top left), the additional monthly evapotranspiration totals are small and limited to the main vegetation period from March to September; they only amount to a few mm (yellow and light green colors in the figure). From the middle of the century on values up to 30 mm occur, mainly in the months May until July. In total, for the last decade (2091–2100) over an entire year approximately 685 mm/yr of evapotranspiration losses occur, corresponding to an increase of these losses of 86 mm/yr (14%) with respect to the reference period 1981–2005 (599 mm/yr). This effect is caused only by the A1B climate data forcing, i.e. for today's vegetation coverage. In the used model version, the evapotranspiration processes comprise evaporation and transpiration (as resulting from the Penman-Monteith approach) as well as sublimation of previously intercepted snow (as computed with the new snow-canopy interaction model). We use the term "loss" here in connection with evapotranspiration since it mostly explains the decrease in water availability in terms of streamflow. The annual pattern, and its evolution over the decades until the end of the century, remains similar for the different storylines A, B and C compared to the "Baseline". They only become slightly more accentuated. The maximum of evapotranspiration increase occurs in July during the last decade for C (the green in the figure corresponds to 34–38 mm/month). During this period, the surplus of mean annual evapotranspiration losses would amount to 195 mm/yr, i.e. the evapotranspiration losses hence more than double by the changes in land use in an A1B climate: 109 mm/yr of the mean annual evapotranspiration (2091–2100) are induced only by the modified forest management in the storyline (difference C - "Baseline": 195 mm/yr–86 mm/yr).

In the RCP8.5 scenario, the pattern is generally the same, only the range of the values is larger. The stepwise increase in the mean monthly evapotranspiration totals after the mid of the century is much more significant than in the A1B "Baseline" simulation, reaching approximately 40 mm/month. The maximum increase in evapotranspiration occurs in storyline C for the decade 2081–2090 with 54–58 mm/month in June or 337 mm/yr in the average for this decade, corresponding to an increase of 51% with respect to the reference period 1981–2005 (658 mm/yr). In RCP8.5 the difference to the signal in evapotranspiration induced only by land use change (difference C - "Baseline": 329–218 mm/yr for 2091–2100) amounts to 111 mm/yr.

Finally, we show how changes in seasonal evaporation losses from precipitation intercepted by vegetation are simulated (for the extreme case RCP8.5 only, Fig. 13). For rainfall (left) a reduction can be detected

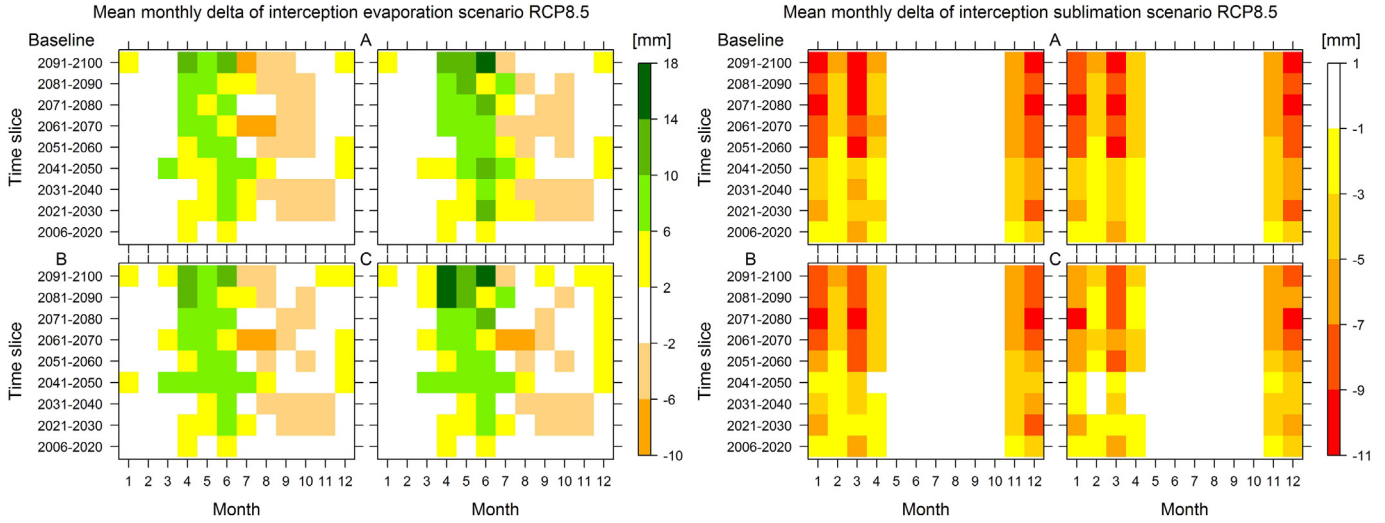

Fig. 13. Mean monthly delta of interception evaporation (difference to the reference period 1981–2005) of liquid precipitation (left) and interception sublimation of solid precipitation (right) for current forest management conditions ("Baseline"), as well as for storylines A, B and C with RCP8.5 climate scenario conditions.

for the summer months (brown colors), whereas for spring the green colors indicate an increase. The latter are caused by the changes in precipitation, both concerning the mean monthly amounts and the shift from snowfall to rainfall events. The maximum increases in the mean monthly values are 14–18 mm/month (e.g. in the last decade and storyline C in April and June); the decrease in summer amounts to 10 mm/month. Mean monthly evaporation totals in spring increase for these decades as a consequence of forest management practice in storylines A to B and C. The reason is the increasing total interception storage for a growing forest area and the seasonal shift of precipitation to the winter months. The increase in the annual evaporation from the liquid water interception storage in the decade 2091–2100 and for storyline C amounts to 65 mm/yr; 22 mm/yr are thereby attributable to climate change (i.e. change in the "Baseline" storyline). Snow sublimation (Fig. 13, right) is naturally limited to the winter months. These losses decrease in the second half of the century by up to 9–11 mm/month on average. The effect of an increasing forest area is hence more than counter-compensated for the process of snow sublimation in a further warming climate (larger interception storage, but less snowfall fraction). In total, sublimation losses from the interception storage in the solid phase decrease by almost 90% until 2091–2100, only 6 mm/yr remain in the last decade (in "Baseline"). Attributable to the growing forest area fraction only in storyline C the interception sublimation amounts to 17 mm/yr for the decade 2091–2100, corresponding to a reduction of 68%.

5. Conclusions and outlook

In most of the existing numerical experiments to the effects of climate change on the hydrological fluxes in a catchment it is assumed that the changing climatic conditions are the only forcing elements that change in the future, whereas other factors of the locally determining framework like the socio-economic development remain steady. Thereby it is mostly unclear if the effects of the socio-economic conditions are (at least) in the same range in their magnitude like the ones of the changing natural environment, or if they even surpass them. Considerable challenges in the assessment of potential future changes of the socio-economic conditions are attributable to the fact that (i) the socio-economic development in the future is not – or only vaguely – predictable for the long term (other than climate which is commonly predicted until the end of the century, even though respective uncertainties are large), and (ii) in contrary to climate, the socio-economic development in the future is much more depending and forced by local and/or regional processes.

In terms of scientific advance, we provide a contribution to scenario development as a method of inter- and transdisciplinary integration of scientific disciplines and the non-scientific community from various societal sectors. An important methodical component thereby is the inter- and transdisciplinary integration of knowledge for the development of the final storylines. Cooperation between meteorologists, sociologists and hydrologists provided the interdisciplinary view necessary to produce the required time series of land use maps used as input for the hydrological modelling.

In the hydrological part of the impact study presented here we made an attempt by means of this intensive local actor process to jointly develop potential futures of socio-economic development which accompany downscaled A1B (moderate) and RCP8.5 (extreme) climate scenarios. These are formulated as so-called "storylines" and quantified into measures to be used in the hydrological modelling as future land use maps and respective plant parameters, as well as continuous time series of meteorological forcing data. In that aspect our methodology is different from most existing approaches in which more or less simple assumptions are made for potential changes in land use going along with a certain changing climate. The storylines in our study are plausible and consistent, i.e. the underlying assumptions are convincing, and free of contradictions. They describe reaction paths to the processes of globalization at the local and regional scale (according to the theory of community resilience after Wilson (2012)), with respective consequences for the patterns of land use and – in particular in our test site, the Brixental in Tyrol/Austria – for the forest management practice. By abandonment of areas previously cultivated as mountain pastures the fraction of forested area can increase, a process that affects the hydrological fluxes. In our experiments for the storylines A, B and C, the forested area increases in the simulations until the end of the century by 6.4% (A1B) or 3.7% (RCP8.5), 16.6% (A1B) or 13.1% (RCP8.5) and 33.4% (A1B) or 29.2% (RCP8.5).

The results of the model simulations for the developed storylines are analyzed such that the effects of a future climate is once determined for steady-state land use conditions ("Baseline"), and for combined future land use and climate evolution. With the latter as the only cause, the mean annual streamflow in the Brixentaler Ache (gauge Bruckhäusl) is reduced by −25% (A1B) and −69% (RCP8.5) until the end of the century. In reality, this would mean massive consequences for the economic and life conditions in the Brixental. Adding the changes in land use as described in the storylines increases the reduction of mean annual streamflow in storyline C up to 35% (A1B) and 77% (RCP8.5) until the end of the century. In absolute values, the reduction of streamflow induced by changing land use only amounts to 99 mm/yr in A1B and 92 mm/yr in RCP8.5 for storyline C. This effect is independent of the climate evolution.

The effect of a changing land use is significantly smaller than the one of climate change for the given area distribution of the land use classes and the assumptions made for the storyline development. RCP8.5 also has to be interpreted as worst case extreme. In catchments with a larger fraction of the formerly cultivated mountain pasture areas that can become overgrown with bushes, and later trees, the relative reduction of streamflow by enhanced evapotranspiration processes could be even more significant.

The change of the seasonal streamflow regime differs with respect to the two used climate scenarios: whereas in A1B the dominant snowmelt processes in spring result in a respective streamflow maximum in spring even in the end of the century, in RCP8.5 the drop in snowfall fraction of precipitation leads to a streamflow maximum in summer. The reduction of streamflow caused by climate change is enhanced by the effect of the changing land use in all months, mainly in the spring and summer of the second half of the century.

Analyses of the decadal and seasonal changes in the modelled evapotranspiration lead to an increase in evapotranspiration losses caused by climate change only (i.e. constant land use) of 86 mm/yr for A1B until the end of the century. If land use changes as well (storyline C), another 109 mm/yr add to that, resulting in 195 mm/yr for the combination of the land use and climate scenarios. For RCP8.5 the increase in the evapotranspiration losses caused by climate change only amount to 218 mm/yr to the end of the century, plus 111 mm/yr for a changing land use. In total these sum up to 329 mm/yr until the end of the century (storyline C).

In the domain of hydrological process modelling we have developed a new module for the open-source, physically based water balance simulation model WaSiM which enables to consider snow-canopy interaction processes and their hydrological consequences in the simulations. Sublimation losses from the interception storage in the canopy are mainly relevant if precipitation occurs in its liquid phase. They increase with climate change in the spring months and can be additionally enhanced if forested areas increase in their extent in the catchment. For the climatic conditions in RCP8.5 the snow interception and sublimation processes are in the same order of magnitude like for the evaporation of liquid precipitation only in the near future. With the decline of the snowfall fraction of precipitation this process will lose its importance. For higher Alpine regions, or in other climate zones, the snow-canopy interaction processes may be of significant importance, though.

Taking all together we can state that a withdrawal and abandonment of formerly cultivated mountain pasture areas with subsequent

afforestation can intensify the reduction of long-term streamflow due to climate change. This effect mainly depends on the fraction and characteristics of the area that is affected by abandonment and subsequent afforestation in the catchment. Vice versa, further care and cultivation of the existing mountain pasture land can represent a contribution to sustainable adaptation to climate change. Balanced management of future regional land use hence provides the potential for coping with the effects of a changing climate in Alpine regions. In no case we question the always existent and valuable ecosystem functions of a forest. It keeps away rockfalls, debris flows and avalanches from the valley floors. Due to the infiltration characteristics of forest soils, peak discharge is usually significantly reduced during flood events in forested catchments (Wahren et al., 2012). In the same time forest protects our drinking water and provides living space to animals and plants. All this was not contested in our mutual learning alliances for joint transdisciplinary scenario development.

Many possibilities for improvement remain in our study along the entire chain of modelling. The used map of the grain size distribution of the soil was assumed to be constant and does not change simultaneously with the land use evolution as prescribed in the storylines. The latter was discretized in the simulations as step-like changes all ten years, rather than as continuous change as in reality.

As climate scenarios we selected only two concrete realizations, since bandwidths and uncertainties of model simulations cannot be used in the transdisciplinary storyline development process. Hence, we used one moderate (A1B) and one extreme (RCP8.5) realization, and chose average climate model realizations with respect to the resulting temperature trends. The uncertainties originating in the simulation of the potential future climate evolution are still significant and add to the ones in the hydrological modelling. More specifically, ET simulation algorithms should be further validated in terms of advanced parameter sets for a wide range of species and to improve the capabilities of the model to predict the hydrological response to climate-induced changes in phenology (Hwang et al., 2018). Future efforts should include a fully coupled dynamic vegetation modelling to account for longer vegetation periods that might even lead to increasing ET and hence additional reduction of streamflow in a warming climate.

The integration of global future climate evolution with local socio-economic development, and means to quantify the respective processes in a numerical hydrological modelling experiment, are new challenges in hydrology. Panta rhei[1] and socio-hydrology (Sivapalan et al., 2012) are the applicable strategic research framing conditions in the community.

Acknowledgements

The presented study was funded by the Austrian Climate Research Program of the Austrian Climate and Energy Fund [project STELLA KR13AC6K11109, ACRP6]. Parts of the WaSiM model development was supported by the Bavarian State Ministry of the Environment and Consumer Protection StMUV [project BIAS II TKP01KPB-66747]. Many supporting people have significantly contributed to the success of the study. Elisabeth Mair, Melanie Steinbacher and Marcel Siegmann (all University of Innsbruck) worked for the project in its beginning and prepared much of the material that was used later on. Stefan Pohl (†), Jakob Garvelmann (both University of Freiburg) and Michael Warscher (IMK-IFU Garmisch-Partenkirchen) helped with processing and interpreting the measurement data. Matthias Themessl, Stefan Ropač, Angelika Wolf and Heide Spitzer (all Climate Change Service Center, Graz/Austria) planned and organized the stakeholder workshops which were moderated by Ines Omann (Vienna) and documented by Viktoria Wegscheider and Carolin Holtkamp (both Innsbruck). We profited from many very valuable supporting ideas and experience of the local actors, forest experts and farming specialists Johann Bachler, Gerhard Markart, Patricia Schrittwieser, Alois Simon, Dieter Stöhr and Peter Zimmermann (all Innsbruck). Finally, Jörg Schulla (Zürich) programmed the WaSiM interface for our new snow-canopy model extension and provided support in its design. Florian Hanzer (University of Innsbruck) helped with debugging of the new code. Meteorological data was provided by the Zentralanstalt für Meteorologie und Geodynamik (Vienna) and the Hydrographic Service of Tyrol (Innsbruck). We greatly acknowledge the contributions of two anonymous reviewers for their comprehensive and constructive improvements of the manuscript of this paper.

Appendix A

Table 1
Description of the 12 coupled scenarios of local land use and climate for the Brixental (with the focus here on the respective implications for forest management).

Relocalized region A relocalized region is based on regional small-scale value chains. Therefore, tourism, agriculture and forestry are focused on internal circular flows. Personal connections and traditional forms of economy are of importance.	**A1B**	In the **resilient** scenario, the forest is mainly dominated by an ecologically mixed cultivation with a harmonious age structure, and it fulfils its different functions. In a **vulnerable** scenario, the forest is mainly dominated by a monoculture and the age structure of the trees is unfavorable.
	RCP8.5	In a **resilient** scenario, the forest is ecologically mixed and trees species are adapted to warmer temperatures. Thereupon it fulfils its different functions. In a **vulnerable** scenario, the mixed cultivation is not enhanced and not adapted to warmer temperatures.
Glocal region A glocal region tempts to combine positive aspects of local and global development attributes. Therefore, local value chains are merged with the global market.	**A1B**	In a **resilient** version of the scenario, the forest is economically used, but even with partly monoculture, an ecologically mixed cultivation dominates. In a **vulnerable** scenario, the forest is dominated by a monoculture and its cultivation and economic function is abandoned.
	RCP8.5	In a **resilient** scenario, the forest is economically used and an ecologically mixed, adapted cultivation is dominant. The forest area extends towards higher altitudes. In a **vulnerable** scenario, a monoculture in the forest is not adapted to the warmer and drier climate.
Super-globalized region A super-globalized region is economically focusing on the global commodity market and forestry reacts on international demand.	**A1B**	In a **resilient** scenario, the economic function of the forest is in focus, however ecological standards are fulfilled. Therefore, the cultivation is mixed and the age structure is in harmony. In a **vulnerable** scenario, the forest is first overexploited and consequently abandoned.
	RCP8.5	In a **resilient** scenario, the warmer temperature is seen as an engine of growth and the cultivation of species is adapted. Even if the economic use of the forest is dominating, it fulfils minimum standards of its other functions. In a **vulnerable** scenario, the forest is overexploited and a young monoculture is dominating the forest.

[1] https://iahs.info/Commissions–W-Groups/Working-Groups/Panta-Rhei.do

Table 2
Performance measures for streamflow simulations achieved for the calibration and validation period for Bruckhäusl gauging station. Values refer to the new WaSiM version including the snow-canopy extension. See Moriasi et al. (2007) for an in-depth review of the used performance measures.

Performance measure	Calibration 2008–2012	Validation 2013–2015
Nash-Sutcliffe efficiency [−]	0.63	0.70
PBIAS [%]	−6.32	−4.02
RMSE [mm/h]	0.05	0.05
RSR [−]	0.61	0.55
Pearson Correlation [−]	0.84	0.84

Table 3
Winter and summer vegetation parameters in WaSiM (albedo α, canopy resistance r_c, leaf area index LAI, roughness length z_0, vegetation cover fraction VCF, and root depth z_R). The parameters have been compiled from various literature sources. See references in the text.

Land use class	Winter values (dormancy)						Summer values						Comments
	α	r_c	LAI	z_0	VCF	z_R	α	r_c	LAI	z_0	VCF	z_R	
	[−]	[s m^{-1}]	[m m^{-1}]	[m]	[−]	[m]	[−]	[s m^{-1}]	[m m^{-1}]	[m]	[−]	[m]	
Water	0.10	–	0.0	0.30	0.00	0.0	0.10	–	0.0	0.30	0.00	0.0	Control file default
Moor	0.15	50	3.0	0.10	0.80	0.2	0.15	20	4.0	0.10	0.80	0.2	Control file default
Grassland	0.25	90	2.0	0.03	0.95	0.3	0.25	55	4.0	0.04	1.00	0.6	Control file default
Trees/Shrubs	0.20	80	3.0	0.20	0.90	0.5	0.20	60	4.0	0.20	0.90	0.5	Control file default
Deciduous forest	0.15	100	1.0	2.00	0.70	1.4	0.15	65	7.0	2.00	0.95	1.4	Control file default
Coniferous forest	0.12	160	7.0	3.00	0.90	1.2	0.12	110	7.0	3.00	0.95	1.2	Updated values according to literature review
Mixed forest	0.15	180	3.0	2.50	0.80	0.8	0.15	120	8.0	2.50	0.92	0.8	Updated values according to literature review
Partially sealed	0.20	100	1.0	1.00	0.50	0.2	0.20	100	1.0	1.00	0.50	0.2	Control file default
Sealed	0.20	100	1.0	1.00	0.20	0.2	0.20	100	1.0	1.00	0.20	0.2	Control file default
Horticulture	0.25	100	0.5	0.40	0.75	0.8	0.25	60	5.0	3.00	0.75	0.8	Control file default
Mountain pasture	0.25	90	2.0	0.03	0.95	0.3	0.25	55	4.0	0.04	1.00	0.5	Adopted from grassland
Skiing area	0.25	90	2.0	0.03	0.95	0.3	0.25	55	4.0	0.04	1.00	0.5	Copy of mountain pasture
Spruce and fir	0.05	100	7.0	3.00	0.82	0.8	0.08	75	7.0	3.00	0.95	0.8	Like spruce with slightly higher density
Spruce	0.05	100	7.0	3.00	0.80	0.8	0.08	75	7.0	3.00	0.95	0.8	Updated values according to literature review
Douglas fir	0.08	100	8.5	3.00	0.80	1.0	0.10	90	8.5	3.00	0.95	1.0	Updated values according to literature review
Green alder	0.10	100	1.0	0.50	0.70	0.7	0.18	50	4.5	0.50	0.90	0.7	Updated values according to literature review
Mountain pine	0.08	70	4.0	2.50	0.80	0.8	0.11	40	4.0	2.50	0.80	0.8	Updated values according to literature review Very low rc adopted from *Pinus sylvestris*
Swiss stone pine	0.08	120	3.5	2.50	0.50	0.5	0.11	100	3.5	2.50	0.50	0.7	rc from literature. Remainder guess based on other classes. Single trees/low VCF.

References

Adams, M., Markart, G., Stary, U., 2010. A Comparison of Hydrological Models for Forest Management and Climate Change - How Can Existing Models Capture and Reproduce Hydrological Effects of Forests? Department of Natural Hazards and Alpine Timberline, Federal Research and Training Centre for Forests, Natural Hazards and Landscaper (BFW), Innsbruck, Austria

Arnold, D., Schicker, I., Formayer, H., Seibert, P., 2012. Towards high-resolution environmental modelling in the Alpine region. In: Steyn, Douw G., Trini Castelli, S. (Eds.), Air Pollution Modeling and its Application XXI. Springer, Dordrecht, pp. 269–272 (ISBN 978-94-007-1358).

Bay-Larsen, I., Hovelsrud, G., 2017. Activating adaptive capacities: fishing communities in Northern Norway. In: Fondahl, G., Wilson, G.N. (Eds.), Northern Sustainabilities: Understanding and Addressing Change in the Circumpolar World. Springer International Publishing, Cham, pp. 123–134.

Beckers, J., Pike, R., Werner, A.T., Redding, T., Smerdon, B., Anderson, A., 2009a. Hydrologic models for forest management applications: Part 2: Incorporating the effects of climate change. Watershed Manag. Bull. 13, 45–54.

Beckers, J., Smerdon, B., Redding, T., Anderson, A., Pike, R., Werner, A.T., 2009b. Hydrologic models for forest management applications: Part 1: Model selection. Watershed Manag. Bull. 13, 35–44.

Bie, W., Casper, M.C., Reiter, P., Vohland, M., 2015. Surface resistance calibration for a hydrological model using evapotranspiration retrieved from remote sensing data in Nahe catchment forest area. Proc. Int. Assoc. Hydrol. Sci. 368, 81–86. https://doi.org/10.5194/piahs-368-81-2015.

Birkinshaw, S.J., Bathurst, J.C., Robinson, M., 2014. 45 years of non-stationary hydrology over a forest plantation growth cycle, Coalburn catchment, Northern England. J. Hydrol. 519, 559–573. https://doi.org/10.1016/j.jhydrol.2014.07.050.

Bormann, H., Breuer, L., Gräff, T., Huisman, J.A., 2007. Analysing the effects of soil properties changes associated with land use changes on the simulated water balance: a comparison of three hydrological catchment models for scenario analysis. Ecol. Model. 209 (1), 29–40. https://doi.org/10.1016/j.ecolmodel.2007.07.004.

Breuer, L., Eckhardt, K., Frede, H.-G., 2003. Plant parameter values for models in temperate climates. Ecol. Model. 169, 237–293.

Calder, I.R., 1993. Hydrologic effects of land use change. In: Maidment, D.R. (Ed.), Handbook of Hydrology. McGraw-Hill, New York (Chapters 13.1–13.5).

Cullmann, J., Mishra, V., Peters, R., 2006. Flow analysis with WaSiM-ETH – model parameter sensitivity at different scales. Adv. Geosci. 9, 73–77. https://doi.org/10.5194/adgeo-9-73-2006.

Cuo, L., Lettenmaier, D.P., Alberti, M., Richey, J.E., 2009. Effects of a century of land cover and climate change on the hydrology of the Puget Sound basin. Hydrol. Process. 23, 907–933. https://doi.org/10.1002/hyp.7228.

Daanen, R.P., Nieber, J.L., 2009. Coupled liquid water flow and heat transport with phase change in a snowpack. J. Cold Reg. Eng. 23 (2), 43–68. https://doi.org/10.1061/(ASCE)0887-381X(2009)23:2(43).

Debele, B., Srinivasan, R., Parlange, J.Y., 2007. Accuracy evaluation of weather data generation and disaggregation methods at finer timescales. Adv. Wat. Res. 30 (5), 1286–1300.

Déqué, M., 2007. Frequency of precipitation and temperature extremes over France in an anthropogenic scenario: model results and statistical correction according to observed values. Glob. Plan. Ch. 57 (1–2), 16–26.

Dickerson-Lange, S.E., Gersonde, R.F., Hubbart, J.A., Link, T.E., Nolin, A.W., Perry, G.H., Roth, T.R., Wayand, N.E., Lundquist, J.D., 2017. Snow disappearance timing is dominated by forest effects on snow accumulation in warm winter climates of the Pacific Northwest, United States. Hydrol. Process. 31, 1846–1862. https://doi.org/10.1002/hyp.11144.

Donner, L.J., Wyman, B., Hemler, R.S., Horowitz, L.W., Ming, Y., Zhao, M., Golaz, J., Ginoux, P., Lin, S.-J., Schwarzkopf, M.D., Austin, J., Alaka, G., Cooke, W.F., Delworth, T.L., Stuart, F., Gordon, C.T., Griffies, S.M., Held, I.M., Hurlin, W.J., Klein, S.A., Knutson, T.R., Langenhorst, A.R., Lee, H.C., Lin, Y., Magi, B.I., Malyshev, S., Milly, P.C.D., Naik, V., Nath, M.J., Pincus, R., Ploshay, J.J., Ramaswamy, V., Seman, C.J., Shevliakova, E., Sirutis, J.J., Stern, W.F., Stouffer, R.J., Wilson, R.J., Winton, M., Wittenberg, A.T., Fanrong Zeng, F., 2011. The dynamical core, physical parameterizations, and basic simulation characteristics of the atmospheric component AM3 of the GFDL global coupled model CM3. J. Clim. 24 (13), 3484–3519. https://doi.org/10.1175/2011JCLI3955.1.

Dunn, S., Mackay, R., 1995. Spatial variation in evapotranspiration and the influence of land use on catchment hydrology. J. Hydrol. 171, 49–73.

Ewert, F., Rounsevell, M.D.A., Reginster, I., Metzger, M., Leemans, R., 2005. Technology development and climate change as drivers of future agricultural land use. In: Brouwer, F., McCarl, B. (Eds.), Rural Lands, Agriculture and Climate Beyond 2015: Usage and Management Responses. Springer, New York, p. 2006.

Federal Province of Tyrol, 2009. Aktuelle Waldvegetation nach Schiechtl/Stern für Tirol. https://www.data.gv.at/katalog/dataset/af193b31-303e-4dfb-b90d-347ee8e8accb, Accessed date: 11 October 2018.

Federal Province of Tyrol, 2012. Landnutzung Tirol. https://www.data.gv.at/katalog/dataset/0eaa80ce-5156-4043-aeab-77f2b24b76b5, Accessed date: 11 October 2018.
Federal Province of Tyrol, 2017. Flächendaten des Landes Tirol. https://www.tirol.gv.at/statistik-budget/statistik/flaechennutzung/, Accessed date: 11 October 2018.
Federal Province of Tyrol, 2018. Laserscan data of Tyrol. https://www.tirol.gv.at/sicherheit/geoinformation/geodaten/laserscandaten/, Accessed date: 11 October 2018.
Federer, C., Vörösmarty, C., Fekete, B., 1996. Intercomparison of methods for calculating potential evaporation in regional and global water balance models. Water Resour. Res. 32, 2315–2321.
Förster, K., Garvelmann, J., Meißl, G., Strasser, U., 2018. Modelling forest snow processes with a new version of WaSiM. Hydrol. Sci. J. https://doi.org/10.1080/02626667.2018.1518626 (accepted manuscript).
Gasser, D., Hauser, L., Quirici, R., Preuschoff, P., Schlaäpfer, M., Wegmann, R., Kleinn, J., Verbunt, M., Gurtz, J., Schär, C., Wehrli, B., 2003. Einfluss von Klima- und Landnutzungsänderungen auf den Abfluss der Thur. Gruppe "Klima und Hydrologie" der Fallstudie Thur, ETH Zürich. WEL. 95 pp. 337–343.
Gelleszun, M., Kreye, P., Meon, G., 2017. Representative parameter estimation for hydrological models using a lexicographic calibration strategy. J. Hydrol. 553, 722–734. https://doi.org/10.1016/j.jhydrol.2017.08.015.
Goler, R.A., Formayer, H., 2012. Temporal disaggregation of daily meteorological data to 15-minute intervals for use in hydrological models. EMS Annual Meeting Abstracts. Vol. 9 EMS2012-174-1. http://meetingorganizer.copernicus.org/EMS2012/EMS2012-174-1.pdf, Accessed date: 11 October 2018.
Green, W.H., Ampt, G., 1911. Studies on soil Phyics. J. Agricul. Sci. 4 (1), 1–24. https://doi.org/10.1017/S0021859600001441.
Haiden, T., Kann, A., Wittmann, C., Pistotnik, G., Bica, B., Gruber, C., 2011. The integrated nowcasting through comprehensive analysis (INCA) system and its validation over the eastern alpine region. Weather Forecast. 26 (2), 166–183. https://doi.org/10.1175/2010WAF2222451.1.
Hiebl, J., Frei, C., 2016. Daily temperature grids for Austria since 1961—concept, creation and applicability. Theor. Appl. Climatol. 124 (1–2), 161–178.
Hotter, M., Simon, A., Vacik, H. (Eds.), 2015. Waldtypisierung Tirol. Amt der Tiroler Landesregierung, Innsbruck 2015.
Hwang, T., Martin, K.L., Vose, J.M., Wear, D., Miles, B., Kim, Y., Band, L.E., 2018. Nonstationary hydrologic behavior in forested watersheds is mediated by climate-induced changes in growing season length and subsequent vegetation growth. Water Resour. Res. 54, 5359–5375. https://doi.org/10.1029/2017WR022279.
Hydrographic Service of Tyrol, 2018. Hydro Online, das Online-Angebot des Hydrographischen Dienstes Tirol. https://www.tirol.gv.at/umwelt/wasser/wasserkreislauf/hydro-online/, Accessed date: 11 October 2018.
Isotta, F.A., Frei, C., Weilguni, V., Perčec Tadić, M., Lassegues, P., Rudolf, B., Pavan, V., Cacciamani, C., Antolini, G., Ratto, S.M., Munari, M., Micheletti, S., Bonati, V., Lussana, C., Ronchi, C., Panettieri, E., Marigo, G., Vertacnik, G., 2014. The climate of daily precipitation in the Alps: development and analysis of a high-resolution grid dataset from pan-Alpine rain-gauge data. Int. J. Climatol. 34 (5), 1657–1675.
Klöcking, B., Haberlandt, U., 2002. Impact of land use changes on water dynamics – a case study in temperate meso and macroscale river basins. Phys. Chem. Earth 27, 619–629.
Köplin, N., Schädler, B., Viviroli, D., Weingartner, R., 2013. The importance of glacier and forest change in hydrological climate-impact studies. HESS 17 (2), 619–635. https://doi.org/10.5194/hess-17-619-2013.
Körner, C., Scheel, J.A., Bauer, H., 1979. Maximum leaf diffusive conductance in vascular plants. Photosynthesis. 13, pp. 45–82.
Koutsoyiannis, D., 2003. Rainfall disaggregation methods: theory and applications. Proceedings of the Workshop on Statistical and Mathematical Methods for Hydrological Analysis. Universita degli Studi di Roma La Sapienza, Rome, pp. 1–23.
Kraller, G., Warscher, M., Kunstmann, H., Vogl, S., Marke, T., Strasser, U., 2012. Water balance estimation in high Alpine terrain by combining distributed modeling and a neural network approach (Berchtesgaden Alps, Germany). HESS 16 (7), 1969–1990. https://doi.org/10.5194/hess-16-1969-2012.
Kröger, M., Schäfer, M., 2016. Scenario development as a tool for interdisciplinary integration processes in sustainable land use research. Futures 84 (A), 64–81.
Kunstmann, H., Stadler, C., 2005. High resolution distributed atmospheric-hydrological modelling for Alpine catchments. J. Hydrol. 314 (1–4), 105–124. https://doi.org/10.1016/j.jhydrol.2005.03.033.
Lahmer, W., Pfützner, B., Becker, A., 2001. Assessment of land use and climate change impacts on the mesoscale. Phys. Chem. Earth B 26, 565–575.
Leitinger, G., Ruggenthaler, R., Hammerle, A., Lavorel, S., Schirpke, U., Clement, J., Lamarque, P., Obojes, N., Tappeiner, U., 2015. Impact of droughts on water provision in managed alpine grasslands in two climatically different regions of the Alps. Ecohydrology 8, 1600–1613. https://doi.org/10.1002/eco.1607.
Liston, G.E., Elder, K., 2006. A distributed snow-evolution modeling system (SnowModel). J. Hydrometeorol. 7 (6), 1259–1276. https://doi.org/10.1175/JHM548.1.
Mahat, V., Tarboton, D.G., Molotch, N.P., 2013. Testing above- and below-canopy representations of turbulent fluxes in an energy balance snowmelt model. Water Resour. Res. 49, 1107–1122. https://doi.org/10.1002/wrcr.20073.
Mallampalli, V.R., Mavrommati, G., Thompson, J., Duveneck, M., Meyer, S., Ligmann-Zielinska, A., Gottschalk Druschke, C., Hychka, K., Kenney, M.A., Kok, K., Borsuk, M.E., 2016. Methods for translating narrative scenarios into quantitative assessments of land use change. Environ. Model Softw. 82, 7–20.
Markart, G., Perzl, F., Klebinder, K., Kohl, B., Adams, M., Sotier, B., Stary, U., Strasser, M., Suntinger, K., 2012. Evaluation and quantification of possible impacts of climate change on hydrological characteristics of forests in the Waidhofen ad Ybbs region. Final Rep. CC-WaterS-Clim. Change Impacts Water Supply. Bundesforschungszentrum Ffür Wald, Vienna Austria.
Meißl, G., Formayer, H., Klebinder, K., Kerl, F., Schöberl, F., Geitner, C., Markart, G., Leidinger, D., Bronstert, A., 2017. Climate change effects on hydrological system conditions influencing generation of storm runoff in small Alpine catchments. Hydrol. Process. 31, 1314–1330. https://doi.org/10.1002/hyp.11104.
Michalakes, J., Chen, S., Dudhia, J., Hart, L., Klemp, J., Middlecoff, J., Skamarock, W., 2001. Development of a next generation regional weather research and forecast model. In: Zwieflhofer, W., Kreitz, N. (Eds.), Developments in Teracomputing: Proceedings of the Ninth ECMWF Workshop on the Use of High Performance Computing in Meteorology. World Scientific, Singapore, pp. 269–276.
Monteith, J.L., 1965. Evaporation and the environment. Symp. Soc. Expl. Biol. 19, 205–234.
Moriasi, D.N., Arnold, J.G., van Liew, M.W., Bingner, R.L., Harmel, R.D., Veith, T.L., 2007. Model evaluation guidelines for systematic quantification of accuracy in watershed simulations. Trans. ASABE 50 (3), 885–900.
Nadezhdina, N., Urban, J., Čermák, J., Nadezhdin, V., Kantor, P., 2014. Comparative study of long-term water uptake of Norway spruce and Douglas-fir in Moravian upland. J. Hydrol. Hydromech. 62, 1–6.
Nakicenovic, N., Swart, R. (Eds.), 2000. IPCC Special Report on Emission Scenarios. IPCC, Cambridge University Press, The Edinburgh Building Shaftesbury Road, Cambridge, England 570 p. Summary for policy makers. https://www.ipcc.ch/pdf/special-reports/spm/sres-en.pdf, Accessed date: 11 October 2018.
Nash, J.E., Sutcliffe, J.V., 1970. River flow forecasting through conceptual models, a discussion of principles. J. Hydrol. 227, 33–51.
Natkhin, M., Steidl, J., Dietrich, O., Dannowski, R., Lischeid, G., 2012. Differentiating between climate effects and forest growth dynamics effects on decreasing groundwater recharge in a lowland region in Northeast Germany. J. Hydrol. 448, 245–254. https://doi.org/10.1016/j.jhydrol.2012.05.005.
Niehoff, D., Fritsch, U., Bronstert, A., 2002. Land-use impacts on storm-runoff generation: scenarios of land-use change and simulation of hydrological response in a meso-scale catchment in SW-Germany. J. Hydrol. 267 (1–2), 80–93. https://doi.org/10.1016/S0022-1694(02)00142-7.
Nilsson, A.E., Bay-Larsen, I., Carlsen, H., van Oort, B., Bjørkan, M., Jylhä, K., Klyuchnikova, E., Masloboev, V., van der Watt, L.-M., 2017. Towards extended shared socioeconomic pathways. A combined participatory bottom-up and top-down methodology with results from the Barents region. Glob. Environ. Chang. 45, 124–132.
Radu, R., Déqué, M., Somot, S., 2008. Spectral nudging in a spectral regional climate model. Tellus Ser. A Dyn. Meteorol. Oceanogr. 60, 898–910. https://doi.org/10.1111/j.1600-0870.2008.00341.x.
Reed, M.S., Kenter, J., Bonn, A., Broad, K., Burt, T.P., Fazey, I.R., Frazer, E.D.G., Hubacek, K., Nainggolan, D., Quinn, C.H., Stringer, L.C., Ravera, F., 2013. Participatory scenario development for environmental management: a methodological framework illustrated with experience from the UK uplands. J. Environ. Manag. 128, 345–362.
Reginster, I., Rounsevell, M.D.A., 2003. Land use change scenarios for Europe. Land Use Land Cover Change Newsl. 9, pp. 10–11.
Richards, L.A., 1931. Capillary conduction of liquids through porous mediums. J. Appl. Phys. 1 (5), 318–333. https://doi.org/10.1063/1.1745010.
Schermer, M., Stotten, R., Strasser, U., Meissl, G., Förster, K., Marke, T., Formayer, H., 2018. The role of transdisciplinary research for agricultural climate change adaptation strategies. Agronomy, Spec. Iss. "Climate Change in Agriculture: Impacts and Adaptations" (in review).
Schirpke, U., Kohler, M., Leitinger, G., Fontana, V., Tasser, E., Tappeiner, U., 2017. Future impacts of changing land-use and climate on ecosystem services of mountain grassland and their resilience. Ecosyst. Serv. 26, 79–94. https://doi.org/10.1016/j.ecoser.2017.06.008.
Schulla, J., 1997. Hydrologische Modellierung von Flussgebieten zur Abschätzung der Folgen von Klimaänderungen. Thesis (PhD). ETH Zürich.
Schulla, J., 2015. Model Description WaSiM (Water Balance Simulation Model) - Completely Revised Version of 2012 With 2013 to 2015 Extensions. Hydrology Software Consulting, J. Schulla. http://www.wasim.ch/downloads/doku/wasim/wasim_2013_en.pdf, Accessed date: 11 October 2018.
Sivapalan, M., Savenije, H.H.G., Blöschl, G., 2012. Socio-hydrology: a new science of people and water. Hydrol. Process. 26 (8), 1270–1276. https://doi.org/10.1002/hyp.8426.
Stotten, R., Schermer, M., Strasser, U., Meißl, G., Marke, T., Förster, K., Formayer, H., 2018. Participatory Socio-Economic Scenarios for Land Use Change: A Methodological Approach. Proc. 13th European IFSA Symp. (Chania/Greece) , pp. 1–13. http://www.ifsa2018.gr/uploads/attachments/113/Theme3_Stotten.pdf, Accessed date: 11 October 2018.
Strasser, U., Etchevers, P., 2005. Simulation of daily discharges for the upper durance catchment (French alps) using subgrid parametrization for topography and a forest canopy climate model. Hydrol. Process. 19 (12), 2361–2373. https://doi.org/10.1002/hyp.5889.
Strasser, U., Warscher, M., Liston, G.E., 2011. Modelling snow-canopy processes on an idealized mountain. J. Hydrometeorol. 12 (4), 663–677. https://doi.org/10.1175/2011JHM1344.1.
Strickler, A., 1923. Beiträge zur Frage der Geschwindigkeitsformel und der Rauhigkeitszahlen für Ströme, Kanäle und geschlossene Leitungen. Mitteilungen des Amtes für Wasserwirtschaft 16, Bern, Eidg. Amt für Wasserwirtschaft.
Tappeiner, U., Tasser, E., Leitinger, G., Tappeiner, A.C.G., 2008. Effects of historical and likely future scenarios of land use on above- and belowground vegetation carbon stocks of an Alpine Valley. Ecosystems 11, 1383–1400.
Tasser, E., Walde, J., Tappeiner, U., Teutsch, A., Noggler, W., 2007. Land-use changes and natural reforestation in the Eastern Central Alps. Agric. Ecosyst. Environ. 118 (1–4), 115–129.
Tasser, E., Schermer, M., Siegl, G., Tappeiner, U., 2012. Wir Landschaftmacher. Vom Sein und werden der Kulturlandschaft in Nord-, Ost- und Südtirol. Athesia, Bozen (264 p).
Tenhunen, J., Geyer, R., Adiku, S., Reichstein, M., Tappeiner, U., Bahn, M., Cernusca, A., Dinh, N.Q., Kolcun, O., Lohila, A., Otieno, D., Schmidt, M., Schmitt, M., Wang, Q.,

Wartinger, M., Wohlfahrt, G., 2009. Influences of changing land use and CO_2 concentration on ecosystem and landscape level carbon and water balances in mountainous terrain of the Stubai Valley, Austria. Glob. Planet. Chang. 67, 29–43.
Tomer, M.D., Schilling, K.E., 2009. A simple approach to distinguish land-use and climate-change effects on watershed hydrology. J. Hydrol. 376 (1–2), 24–33. https://doi.org/10.1016/j.jhydrol.2009.07.029.
Van Vuuren, D.P., Carter, D.R., 2014. Climate and socio-economic scenarios for climate change research and assessment: reconciling the new with the old. Clim. Chang. 122, 415–429. https://doi.org/10.1007/s10584-013-0974-2.
Van Vuuren, D.P., Edmonds, J., Kainuma, M., Riahi, K., Thomson, A., Hibbard, K., Hurtt, G.C., Kram, T., Krey, V., Lamarque, J.-F., Masui, T., Meinshausen, M., Nakivenovic, N., Smith, S.J., Rose, S.K., 2011. The representative concentration pathways: an overview. Clim. Chang. 109 (1–2), 5–31. https://doi.org/10.1007/s10584-011-0148-z.
Varhola, A., Coops, N.C., Weiler, M., Moore, R.D., 2010. Forest canopy effects on snow accumulation and ablation: an integrative review of empirical results. J. Hydrol. 392, 219–233. https://doi.org/10.1016/j.jhydrol.2010.08.009.
Wahren, A., Schwärzel, K., Feger, K.-H., 2012. Potentials and limitations of natural flood retention by forested land in headwater catchments: evidence from experimental and model studies. J. Flood Risk Man. 5 (4), 321–335.
Walz, A., Lardelli, C., Behrendt, H., Grêt-Regamey, A., Lundström, C., Kytzia, S., Bebi, P., 2007. Participatory scenario analysis for integrated regional modelling. Landsc. Urb. Plann. 81 (1–2), 114–131.
Warscher, M., Strasser, U., Kraller, G., Marke, T., Franz, H., Kunstmann, H., 2013. Performance of complex snow cover descriptions in a distributed hydrological model system - a case study for the high alpine terrain of the berchtesgaden alps. Water Resour. Res. 49, 2619–2637. https://doi.org/10.1002/wrcr.20219.
Wilson, G.A., 2012. Community resilience, globalization, and transitional pathways of decision-making. Geoforum 43, 1218–1231.
Zierl, B., Bugmann, H., 2005. Global change impacts on hydrological processes in Alpine catchments. Water Resour. Res. 41, W02028. https://doi.org/10.1029/2004WR003447.